Geochemistry and U-Pb zircon geochronology of mid-Cretaceous Tay River suite intrusions in southeast Yukon

***Lee C. Pigage*[1]**
Yukon Geological Survey

Jim L. Crowley
Department of Geosciences, Boise State University

Charlie F. Roots
Geological Survey of Canada

J. Grant Abbott
Yukon Geological Survey

Pigage, L.C., Crowley, J.L., Roots, C.F., and Abbott, J.G., 2014. Geochemistry and U-Pb zircon geochronology of mid-Cretaceous Tay River suite intrusions in southeast Yukon. *In:* Yukon Exploration and Geology 2014, K.E. MacFarlane, M.G. Nordling, and P.J. Sack (eds.), Yukon Geological Survey, p. 169-194.

ABSTRACT

Reconnaissance geological mapping in the Coal River map area of southeastern Yukon investigated several small mid-Cretaceous plutons. The intrusions are composed of unfoliated or incipiently foliated, fine to coarse-grained, equigranular and porphyritic, biotite ± hornblende quartz monzodiorite to granodiorite. They are metaluminous to peraluminous and have reduced to oxidized geochemical characteristics. The composition of selected samples is consistent with magma formation from partial melting of infracrustal source rocks.

U-Pb ages were obtained for nine plutons from five or six zircon single-grain analyses by the isotope dilution thermal ionization mass spectrometry method with chemical abrasion (CA-TIMS). All interpreted ages are concordant within statistical uncertainty. The plutons range in age from 99.80 ± 0.03 to 97.70 ± 0.03 Ma. Given the primarily unfoliated nature of the plutons, contractional, fabric-forming deformation within the Cordilleran orogeny must therefore have largely ceased at the present level of exposure in the Coal River area by the time of intrusion (*ca.* 98 Ma).

The ages and compositions of the plutons in Coal River map area are consistent with their being part of the Tay River plutonic suite, a northwest-trending belt of coeval and compositionally similar plutons and local volcanic rocks (South Fork volcanic suite) that, when augmented by the addition of the Coal River plutons, extends approximately 465 km with a width of up to 150 km.

[1] *lee.pigage@gov.yk.ca*

INTRODUCTION

Several metallogenic belts of mid to late-Cretaceous intrusions extend from central Alaska across to southeast Yukon. Informally termed the Tintina gold belt (Smith, 2000), these intrusive belts have been a major impetus for recent exploration in Alaska and Yukon. Intrusions in the Coal River map area (NTS 95D) of southeastern Yukon (Fig. 1) define the most southern exposures of these mid to Late Cretaceous felsic plutons (Northern Cordilleran mid-Cretaceous plutonic province of Hart *et al.*, 2004) northeast of the Tintina fault in Yukon. The intrusions have been classified primarily in terms of age and composition (Pigage and Anderson, 1985; Gordey and Anderson, 1993; Mortensen *et al.*, 1995; 2000; Hart *et al.*, 2004; Heffernan, 2004; Rasmussen *et al.*, 2007; Rasmussen, 2013); these attempts have produced a complex and partially conflicting terminology that includes the Selwyn, Tombstone, Mayo, Tungsten, Tay River, transitional Tungsten-Tay River, Anvil, and Hyland suites.

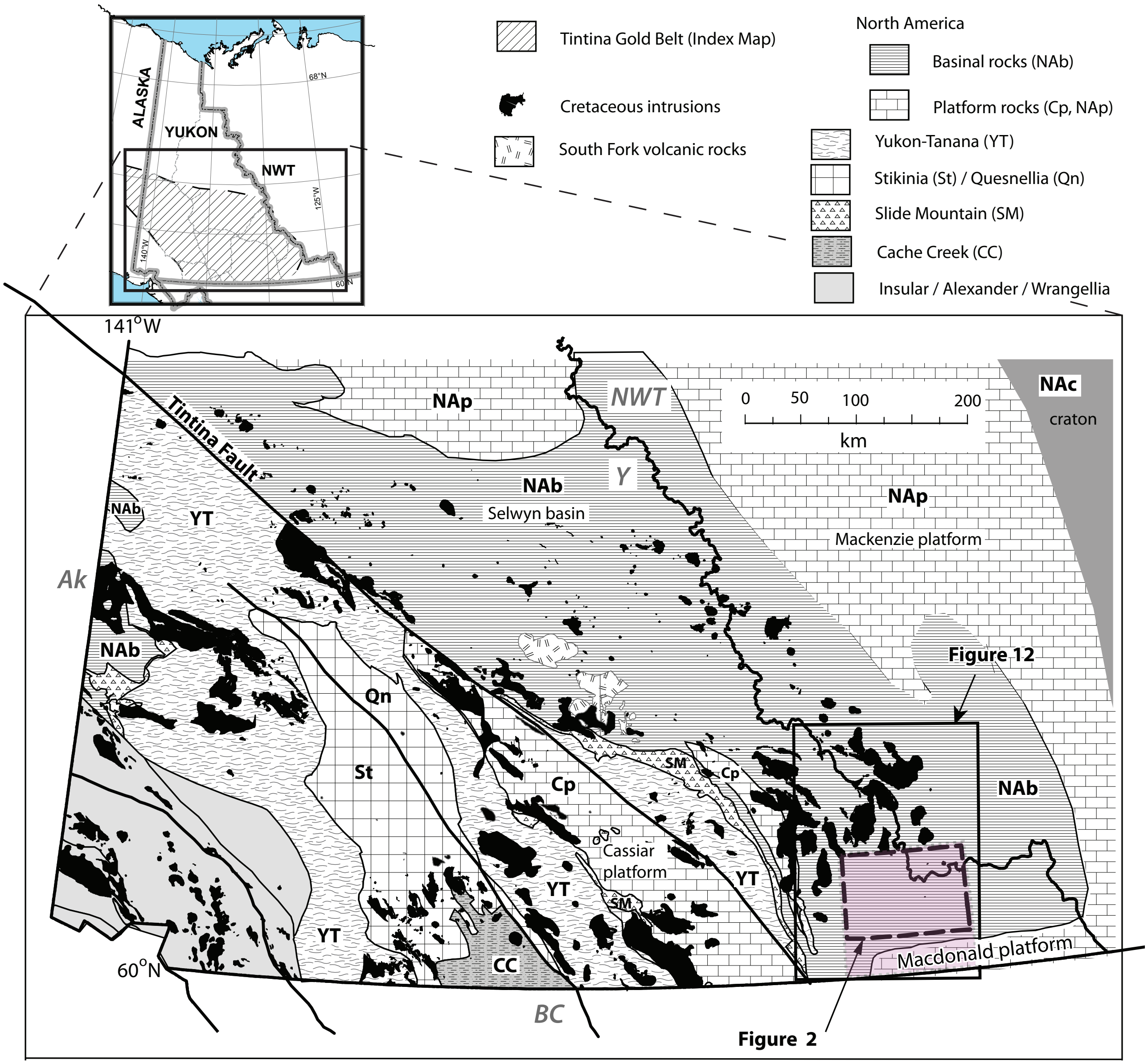

Figure 1. *Cretaceous plutonic rocks in south and central Yukon. The extent of the informal Tintina gold belt (hachured in inset map) is modified from Smith (2000). Distribution of terranes is from Colpron and Nelson (2011) and intrusions from Gordey and Makepeace (2003). Locations of figures 2 (Coal River map area shaded in pink) and 12 are indicated. Abbreviations are: Y=Yukon; NWT=Northwest Territories; BC=British Columbia.*

Bedrock geological mapping (1:250 000 scale) in 2009 and 2010 in the Coal River map area identified several small, previously unrecognized granitoid intrusions. In this paper we document the compositions and ages of many of these intrusions and use these new data to assign them to one of the regionally defined age/composition belts.

REGIONAL GEOLOGY

Southeastern Yukon is mainly underlain by a succession of Proterozoic to upper Eocene sedimentary rocks with a combined thickness of more than 14 000 m (Gabrielse and Blusson, 1969; Long and Sweet, 1994; Pigage, 2004; 2006; 2008; 2009; Pigage *et al.*, 2011). Coal River map area, centered 150 km northeast of the town of Watson Lake, contains Proterozoic siliciclastic rocks deposited during early rifting of the supercontinent Rodinia, lower Paleozoic carbonate strata of the Macdonald platform and marine shales of Selwyn basin, constituting the west-facing, passive continental miogeocline of Laurentia (Cecile *et al.*, 1997). Upper Paleozoic and lower Mesozoic siliciclastic and carbonate rocks were deposited in a shallow marine basin. Significant depositional hiatuses or subsequent erosion occurred in southeast Yukon during this time interval. Upper Eocene to Oligocene sedimentary rocks occur in a north-trending, extensional, half-graben (Pigage, 2008).

The age of contractional deformation and metamorphism is poorly constrained between early Triassic and late Eocene (Pigage, 2008; 2009), broadly correlative with the Cordilleran orogeny (Nelson and Colpron, 2007). It is manifested as northwest to northeast-trending, east-verging, asymmetric folds and reverse faults (Fig. 2). Metamorphic grade ranges from muscovite-chlorite to biotite-staurolite-garnet zones; with metamorphic grade generally decreasing from west to east. Extensional faults offset the late Eocene-Oligocene sediments, suggesting that at least some movement on normal faults is post-Oligocene.

Cretaceous and younger granitoid plutons intrude both the basinal marine siliciclastic rocks and the platformal carbonate rocks of southeast Yukon.

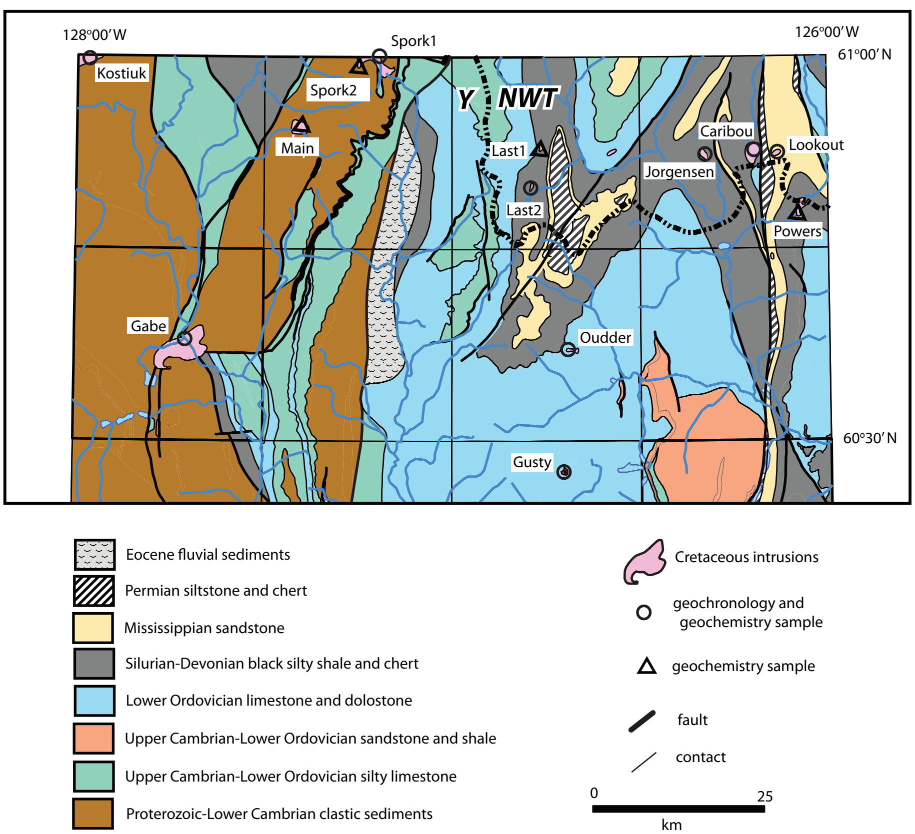

Figure 2. *Locations of samples (coordinates in Table 1) with respect to bedrock geology of northern Coal River map area, modified from Pigage et al. (2011).*

PREVIOUS WORK

Gabrielse and Blusson (1969) completed the first systematic regional mapping program in the Coal River area (based on fieldwork completed in 1967). Subsequent mapping occurred mainly in map areas farther north (*e.g.*, Gabrielse *et al.*, 1973). Pigage and Anderson (1985) and Gordey and Anderson (1993) provided an early framework for defining igneous suites in Selwyn basin and Mackenzie platform of central Yukon. All intrusions were considered to be part of the Selwyn Plutonic Suite (Gordey and Anderson, 1993) or Anvil plutonic suite (Pigage and Anderson, 1985). Mortensen *et al.* (2000) described distinct plutonic suites in central and western Yukon, differentiating them according to spatial distribution, age, lithology, mineralogy and metallogeny. Hart *et al.* (2004) identified 25 Early and mid-Cretaceous plutonic suites and belts extending across Alaska and

Yukon; intrusions in southeast Yukon were assigned to the Anvil-Hyland-Cassiar belt. Regional studies by Heffernan (2004), Rasmussen *et al.* (2007), and Rasmussen (2013) included previously-mapped intrusions in the northeastern corner of the Coal River map area and completed petrological, geochemical, and geochronological analyses. They correlated southeastern Yukon intrusions with several plutonic suites identified in central Yukon, including Tay River, Tombstone, Mayo, and Tungsten suites.

PLUTONIC ROCKS IN COAL RIVER MAP AREA

Field work to update the earlier reconnaissance geology was completed in 2009 and 2010 (Pigage *et al.*, 2011). Several plutons intruding Neoproterozoic through Mississippian carbonate and siliciclastic strata in northern Coal River map area were investigated. All are poorly to moderately exposed and inferred from the extents of their positive aeromagnetic response to be subcircular, ranging from 0.3 to 8.4 km in diameter (Fig. 3).

The exposed plutonic rocks are grey-weathering and unfoliated to slightly foliated. They range in grain size and texture from fine to coarse-grained and equigranular to (dominantly) porphyritic. Biotite ± hornblende are the predominant primary mafic minerals. Coarse-grained, equigranular variants locally have anhedral to subhedral K-feldspar grains. Porphyritic variants are unfoliated and typically crowded with equant plagioclase phenocrysts up to 5 mm across in a fine-grained, grey matrix. Hornblende, biotite, and minor quartz also occur as phenocrysts in the porphyritic phases. Some of the intrusions are compositionally variable, but internal contacts were not mapped because visits were reconnaissance only. Composite intrusive bodies north of the Coal River map area have been identified (Gordey and Anderson, 1993; Pigage and Anderson; 1985). The appendix provides brief descriptions of the mineralogy and fabric of granitoid samples selected for geochemical analysis and geochronology.

Many of the intrusions are weakly to strongly altered, with chlorite replacing hornblende and biotite and very fine sericite replacing feldspar. Epidote and calcite are locally abundant within the matrix.

The Main pluton is unique in containing primary muscovite. It is a medium-grained, equigranular, foliated, medium gray, plagioclase-quartz-muscovite-tourmaline-garnet granitoid rock.

Details of their full extent, contact relationships and metamorphic effects such as hornfelsing, skarn formation, or alteration remain obscure because the intrusions are poorly exposed.

Average magnetic susceptibility readings (MS) for the various plutons range from 0 to 17.8 (10^{-3} SI units; Table 1). The plutons with high MS values contain fine-grained magnetite and correlate closely with large positive anomalies in the first vertical derivative of the regional aeromagnetic field (Fig. 3). Aeromagnetic anomalies associated with several plutons (e.g., Jorgensen, Last2) do not overlap with the surface extent of the plutons. In this case the anomalies may represent pyrrhotite hornfels, magnetite skarns, or a magnetic portion of the pluton extending into the subsurface. The small and sub-circular aeromagnetic anomalies provide a proxy for the size and shape of the poorly exposed plutons and/

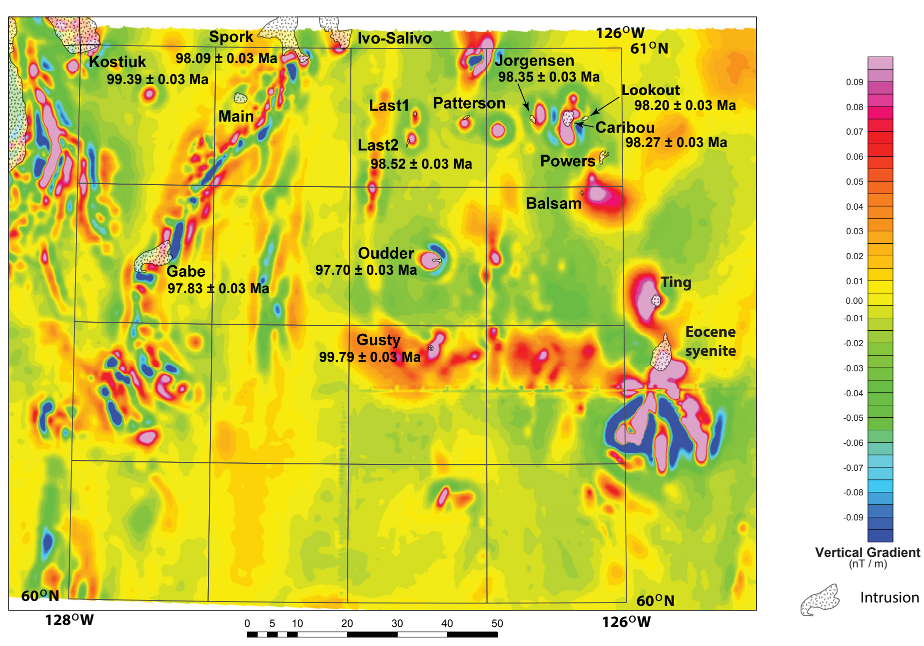

Figure 3. *First vertical derivative of regional aeromagnetic survey, intrusions in Coal River map area are labeled and described in this report. The age labels for the dated plutons have an analytical error of 2 sigma, as described in the text.*

Table 1. *Rock type, texture, magnetic susceptibility, location, and geochemistry of plutons in Coal River map area (NTS 95D). All coordinates NAD83 UTM, Zone 09N.*

Igneous Body		Powers	Jorgensen	Last 2	Gabe	Kostiuk	Oudder	Lookout	Caribou	Last 1	Spork 1	Spork 2	Main	Gusty
Sample #		09RAS137	09RAS136	09LP098	09LP048	09RAS062	09TOA135	09TOA179	09TOA180	09TOA185	10TOA014	10TOA016	10TOA019	Gusty Lake
UTM E		658,872	645,250	620,192	570,761	555,895	625,672	655,673	652,311	621,360	597,672	594,775	586,791	626,261
UTM N		6,743,596	6,751,550	6,745,800	6,722,414	6,762,820	6,723,074	6,752,196	6,752,434	6,751,642	6,764,282	6,762,834	6,754,152	6,704,777
Rock (Fig. 3)		quartz Monzodiorite	quartz monzodiorite	granodiorite	granodiorite	granodiorite	granodiorite	granodiorite	granodiorite	granodiorite	granodiorite	quartz diorite	granite	tonalite
Texture		porphyritic	porphyritic	porphyritic	equigranular	porphyritic	equigranular	porphyritic	porphyritic	porphyritic	equigranular	equigranular	equigranular	porphyritic
Age Date (this paper)		no	yes	yes	yes	yes	yes	yes	yes	no	yes	no	no	yes
M.S.*		0.4	0.2	14.2	1.0	12.1	14.0	0.2	17.8	11.8	5.1	3.3	0.0	0.4
	Anal. Method													
SiO_2 (%)	Fus-ICP	62.65	59.98	61.87	65.83	66.47	65.73	63.28	61.33	65.48	68.22	50.78	74.37	63.87
Al_2O_3 (%)	Fus-ICP	16.90	15.99	16.83	15.86	15.95	15.88	16.09	16.53	16.20	14.97	16.90	14.44	16.53
FeO (%)	Titration	3.65	3.93	3.01	2.69	3.65	2.65	3.44	2.22	2.80	2.49	8.09	0.23	3.00
Fe_2O_3 (%)	calculated	1.36	1.49	1.76	0.47	0.10	1.41	0.70	2.65	0.96	0.66	2.07	1.04	1.11
$Fe_2O_3^T$ (%)	Fus-ICP	5.42	5.86	5.11	3.46	4.16	4.36	4.52	5.12	4.07	3.43	11.06	1.30	4.44
MnO (%)	Fus-ICP	0.086	0.079	0.097	0.075	0.044	0.066	0.086	0.098	0.080	0.067	0.160	0.100	0.054
MgO (%)	Fus-ICP	2.25	2.89	1.92	1.30	1.36	1.68	2.22	2.35	1.77	1.21	3.76	0.07	2.00
CaO (%)	Fus-ICP	3.53	4.55	4.04	3.38	3.50	3.78	3.44	4.49	4.10	3.02	7.63	0.72	5.71
Na_2O (%)	Fus-ICP	4.01	3.77	3.47	2.94	3.36	3.05	3.90	3.46	3.71	3.05	2.89	4.11	2.81
K_2O (%)	Fus-ICP	2.34	2.33	2.29	3.84	3.23	3.91	2.25	2.52	2.50	3.77	1.60	3.79	2.56
TiO_2 (%)	Fus-ICP	0.600	0.840	0.544	0.373	0.537	0.452	0.525	0.553	0.440	0.448	2.526	0.022	0.514
P_2O_5 (%)	Fus-ICP	0.14	0.16	0.15	0.16	0.20	0.29	0.14	0.14	0.13	0.13	0.38	0.07	0.15
L.O.I. (%)	Fus-ICP	2.54	2.53	2.26	0.87	0.83	0.59	4.13	2.62	1.80	1.30	0.98	0.44	1.30
Total		100.06	98.54	98.24	97.79	99.23	99.49	100.20	98.96	99.97	99.34	97.77	99.40	99.61
Au (ppb)	INAA	< 2	< 2	< 2	< 2	< 2	< 2	< 2	< 2	2				
As (ppm)	INAA	< 0.5	< 0.5	1.6	< 0.5	< 0.5	< 0.5	1.3	1.8	< 0.5				
Br (ppm)	INAA	< 0.5	< 0.5	< 0.5	< 0.5	1.6	< 0.5	1.3	< 0.5	< 0.5				
Cr (ppm)	INAA	14	83	15	< 5	9	73	22	35	12				
Ir (ppb)	INAA	< 5	< 5	< 5	< 5	< 5	< 5	< 5	< 5	< 5				
Sc (ppm)	INAA	9.4	12.4	8.6	6.1	7.2	9.3	9.4	10.9	8.0				
Se (ppm)	INAA	< 3	< 3	< 3	< 3	< 3	< 3	< 3	< 3	< 3				
Sb (ppm)	INAA	0.4	< 0.2	0.4	< 0.2	< 0.2	0.2	0.4	0.4	< 0.2				
Sc (ppm)	Fus-ICP	11	13	9	7	8	10	11	12	9	8	29	3	11
Be (ppm)	Fus-ICP	2	2	2	2	2	3	2	2	2	2	1	11	2
V (ppm)	Fus-ICP	106	121	86	59	60	94	90	104	75	60	326	<5	96
Cr (ppm)	Fus-MS	< 20	80	< 20	< 20	< 20	70	< 20	30	< 20	<20	<20	<20	20
Co (ppm)	Fus-MS	9	13	8	5	4	7	8	9	6	5	25	<1	8
Ni (ppm)	Fus-MS	< 20	30	< 20	< 20	< 20	< 20	< 20	< 20	< 20	<20	30	<20	<20
Cu (ppm)	Fus-MS	< 10	10	< 10	< 10	10	< 10	< 10	< 10	< 10	<10	10	<10	50
Zn (ppm)	Fus-MS	110	70	270	40	30	< 30	50	60	40	40	100	50	40
Ga (ppm)	Fus-MS	19	19	18	16	17	17	17	18	17	17	22	21	21
Ge (ppm)	Fus-MS	1.5	1.3	1.5	1.4	1.4	1.7	1.5	1.5	1.5	1.9	2.0	5.2	1.6
As (ppm)	Fus-MS	< 5	< 5	< 5	< 5	< 5	< 5	< 5	< 5	< 5	<5	<5	<5	<5
Rb (ppm)	Fus-MS	71	76	75	135	102	131	68	83	84	136	57	310	71
Sr (ppm)	Fus-ICP	724	622	509	450	344	1064	572	564	502	310	393	17	451
Y (ppm)	Fus-MS	16.9	15.2	18.4	15.3	18.2	22.2	15.3	16.6	16.2	19.1	29.8	20.3	17.5
Zr (ppm)	Fus-MS	160	156	155	167	219	202	147	131	148	160	187	42	141
Nb (ppm)	Fus-MS	16.8	23.0	16.1	16.3	17.7	35.4	15.1	13.0	13.2	16.6	22.8	47.5	10.2
Mo (ppm)	Fus-MS	< 2	< 2	< 2	< 2	< 2	< 2	< 2	< 2	< 2	<2	<2	<2	<2
Ag (ppm)	Fus-MS	< 0.5	< 0.5	< 0.5	< 0.5	0.6	0.5	< 0.5	< 0.5	< 0.5	<0.5	<0.5	<0.5	<0.5

Table 1. *contined.*

Igneous Body		Powers	Jorgensen	Last 2	Gabe	Kostiuk	Oudder	Lookout	Caribou	Last 1	Spork 1	Spork 2	Main	Gusty
Sample #		09RAS137	09RAS136	09LP098	09LP048	09RAS062	09TOA135	09TOA179	09TOA180	09TOA185	10TOA014	10TOA016	10TOA019	Gusty Lake
UTM E		658,872	645,250	620,192	570,761	555,895	625,672	655,673	652,311	621,360	597,672	594,775	586,791	626,261
UTM N		6,743,596	6,751,550	6,745,800	6,722,414	6,762,820	6,723,074	6,752,196	6,752,434	6,751,642	6,764,282	6,762,834	6,754,152	6,704,777
Rock (Fig. 3)		quartz monzodiorite	quartz monzodiorite	granodiorite	granodiorite	granodiorite	granodiorite	granodiorite	granodiorite	granodiorite	granodiorite	quartz diorite	granite	tonalite
Texture		porphyritic	porphyritic	porphyritic	equigranular	porphyritic	equigranular	porphyritic	porphyritic	porphyritic	equigranular	equigranular	equigranular	porphyritic
Age Date (this paper)		no	yes	yes	yes	yes	yes	yes	yes	no	yes	no	no	yes
M.S.*		0.4	0.2	14.2	1.0	12.1	14.0	0.2	17.8	11.8	5.1	3.3	0.0	0.4
	Anal. Method													
In (ppm)	Fus-MS	< 0.1	< 0.1	< 0.1	< 0.1	< 0.1	< 0.1	< 0.1	< 0.1	< 0.1	<0.1	<0.1	<0.1	<0.1
Sn (ppm)	Fus-MS	1	1	2	2	3	2	1	1	2	3	3	7	1
Sb (ppm)	Fus-MS	< 0.2	< 0.2	0.4	< 0.2	< 0.2	< 0.2	< 0.2	< 0.2	< 0.2	<0.2	<0.2	<0.2	<0.2
Cs (ppm)	Fus-MS	2.1	2.7	1.1	3.9	1.2	1.8	1.6	3.6	2.3	2.9	2.2	13.6	2.2
Ba (ppm)	Fus-ICP	892	1077	1093	1303	1164	2050	1530	779	750	766	514	8	623
La (ppm)	Fus-MS	28.7	36.0	33.3	60.8	49.1	81.0	31.1	32.8	32.9	42.7	31.0	6.4	25.4
Ce (ppm)	Fus-MS	55.6	64.7	65.6	109.0	91.1	144.0	58.8	66.3	64.1	77.9	62.7	12.1	49.2
Pr (ppm)	Fus-MS	5.96	7.30	7.08	10.60	9.15	13.90	6.08	7.14	6.82	8.29	7.38	1.29	5.39
Nd (ppm)	Fus-MS	22.1	27.2	25.9	35.8	31.4	47.4	21.9	26.7	24.5	28.6	29.8	4.3	20.5
Sm (ppm)	Fus-MS	4.30	4.30	4.82	5.60	5.19	7.49	3.96	4.88	4.44	5.00	6.28	1.49	3.95
Eu (ppm)	Fus-MS	0.929	1.230	0.954	0.913	0.973	1.280	0.715	1.080	0.928	0.969	1.670	0.078	1.060
Gd (ppm)	Fus-MS	3.64	3.72	3.88	3.99	3.93	5.44	3.26	3.78	3.57	3.53	6.04	1.64	3.56
Tb (ppm)	Fus-MS	0.52	0.55	0.58	0.53	0.57	0.76	0.48	0.56	0.52	0.57	0.98	0.46	0.57
Dy (ppm)	Fus-MS	2.98	3.09	3.36	2.81	3.20	4.06	2.74	3.07	2.92	3.16	5.53	3.14	3.08
Ho (ppm)	Fus-MS	0.58	0.58	0.65	0.53	0.62	0.77	0.54	0.60	0.57	0.63	1.08	0.60	0.63
Er (ppm)	Fus-MS	1.68	1.69	1.90	1.56	1.87	2.26	1.57	1.73	1.65	1.82	3.06	1.89	1.79
Tm (ppm)	Fus-MS	0.253	0.252	0.289	0.232	0.284	0.330	0.241	0.259	0.252	0.276	0.458	0.381	0.283
Yb (ppm)	Fus-MS	1.68	1.62	1.95	1.52	1.95	2.21	1.58	1.69	1.72	1.94	2.94	3.25	1.95
Lu (ppm)	Fus-MS	0.273	0.259	0.312	0.240	0.322	0.349	0.246	0.259	0.267	0.31	0.46	0.63	0.32
Hf (ppm)	Fus-MS	3.6	3.5	3.7	3.7	4.7	4.4	3.5	3.1	3.6	3.9	3.9	2.1	3.4
Ta (ppm)	Fus-MS	1.46	1.14	1.36	1.43	1.66	2.72	1.50	1.41	1.32	1.62	1.88	11.40	0.82
W (ppm)	Fus-MS	< 0.5	< 0.5	2.7	< 0.5	< 0.5	< 0.5	< 0.5	< 0.5	< 0.5	1.3	0.5	0.9	0.9
Tl (ppm)	Fus-MS	0.27	0.27	0.29	0.61	0.44	0.39	0.31	0.29	0.33	0.66	0.27	1.71	0.48
Pb (ppm)	Fus-MS	212	9	29	19	10	14	15	19	13	19	11	33	7
Bi (ppm)	Fus-MS	< 0.1	< 0.1	< 0.1	< 0.1	< 0.1	< 0.1	< 0.1	< 0.1	< 0.1	<0.1	<0.1	2.3	0.3
Th (ppm)	Fus-MS	9.0	9.2	10.1	23.9	16.8	25.4	11.6	12.3	11.2	19.6	6.6	3.7	8.1
U (ppm)	Fus-MS	2.76	2.51	2.70	5.25	2.82	4.64	2.59	2.72	2.71	4.18	1.80	1.36	2.43

whole rock analyses completed at Activation Laboratories Ltd., Ancaster, Ontario in 2009 and 2010

FeO determined by titration

M.S. = magnetic susceptibility (10^{-3} S.I. units) or hornfelsed sediments adjacent to the intrusions. Steep intrusive contacts are suggested by the rapid lateral change in magnetic intensity. Areas with similar positive aeromagnetic patterns in Figure 3 are inferred to mark unmapped or buried intrusions because sedimentary rocks in the map area have low magnetic susceptibilities (MS <1 x 10^{-3} SI units).

A north to northeast-trending, variable but generally positive aeromagnetic anomaly in the western part of the map area (Fig. 3) incorporates the Gabe, Main and Spork plutons. This linear trend is generally coincident with a topographic ridge exposing Neoproterozoic pelites with biotite ± garnet ± staurolite metamorphic assemblages, in contrast to the regional chlorite-muscovite metamorphic grade. Samples from the Gabe and Main intrusions (see Table 1), higher grade metamorphic rocks, and lower grade sedimentary rocks all have weak magnetic susceptibility (≤1 x 10^{-3} SI units). We suggest that this magnetic anomaly trend is likely related to intrusive rocks at depth, either directly as intrusion phases containing magnetite, or indirectly as associated pyrrhotite-bearing hornfels.

Another linear positive magnetic anomaly extends easterly from the Gusty pluton (Fig. 3) to beyond the eastern boundary of the map area where it terminates with a magnetite-bearing, Eocene biotite syenite (described by Pigage, 2009). Scant rock exposure along this aeromagnetic trend are siliciclastic and carbonate rock with little to no magnetic expression. Beneath these strata may be a linear array of unexposed granitoid plutons and associated hornfels. A similar east-trending "string" of magnetic plutons is exposed between the Last1/Last2 and Lookout/Powers plutons.

GEOCHEMISTRY

Thirteen whole rock compositions were determined for 12 plutons within the Coal River map area (Fig 2). Samples are predominantly granodiorite with minor granite, quartz monzodiorite and quartz diorite, based on the proportions of normative minerals (Table 1; Fig. 4a). The common porphyritic texture with a fine-grained, locally extensively altered matrix precludes systematic use of modal compositions (Streckeisen, 1976) to classify many of the intrusions. Samples were examined in thin section; offcuts from the thin sections were etched with HF and stained with sodium cobaltinitrite to estimate the occurrence of K-feldspar (see rock sample descriptions in the Appendix). Rock names were checked where appropriate against approximate mineral modes of stained samples from the particular pluton. Using the MALI classification scheme discussed by Frost *et al.* (2001), the plutons fall within the calc-alkalic suite (Fig. 4b).

SiO_2 (Figs. 5 and 6) for most of the intrusions varies from approximately 60 to 68%; only one sample is mafic (51%), and only the Main pluton is strongly felsic (74%). The Al_2O_3, MgO, $Fe_2O_3^T$ (total iron as Fe_2O_3), and CaO contents decrease approximately linearly with increasing SiO_2. In contrast, K_2O increases with increasing SiO_2, and Na_2O, TiO_2, and P_2O_5 do not show any systematic variation with SiO_2. Trace elements and rare earth elements (Fig. 6) are more scattered, with only V and Sc illustrating linear variation with increasing SiO_2.

Using Shand's index (Fig. 7) the intrusion samples are metaluminous to slightly peraluminous; only the Main

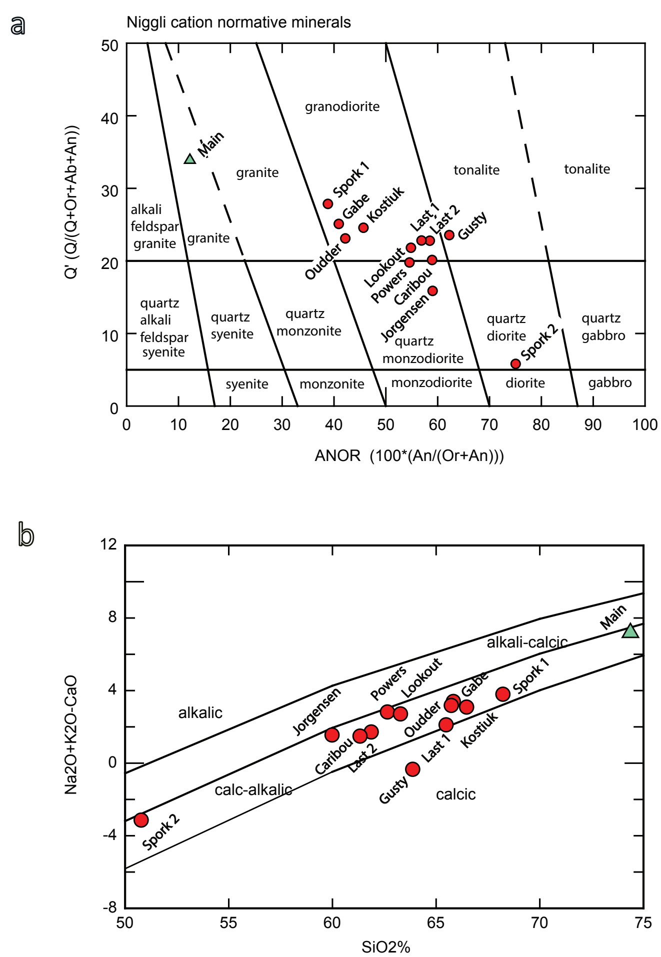

Figure 4. *(a) Compositional classification of igneous plutonic rocks (Streckeisen and Le Maitre, 1979). (b) MALI compositional plot (Frost et al., 2001). The Main intrusion is indicated with a triangle; other intrusions are indicated with circles.*

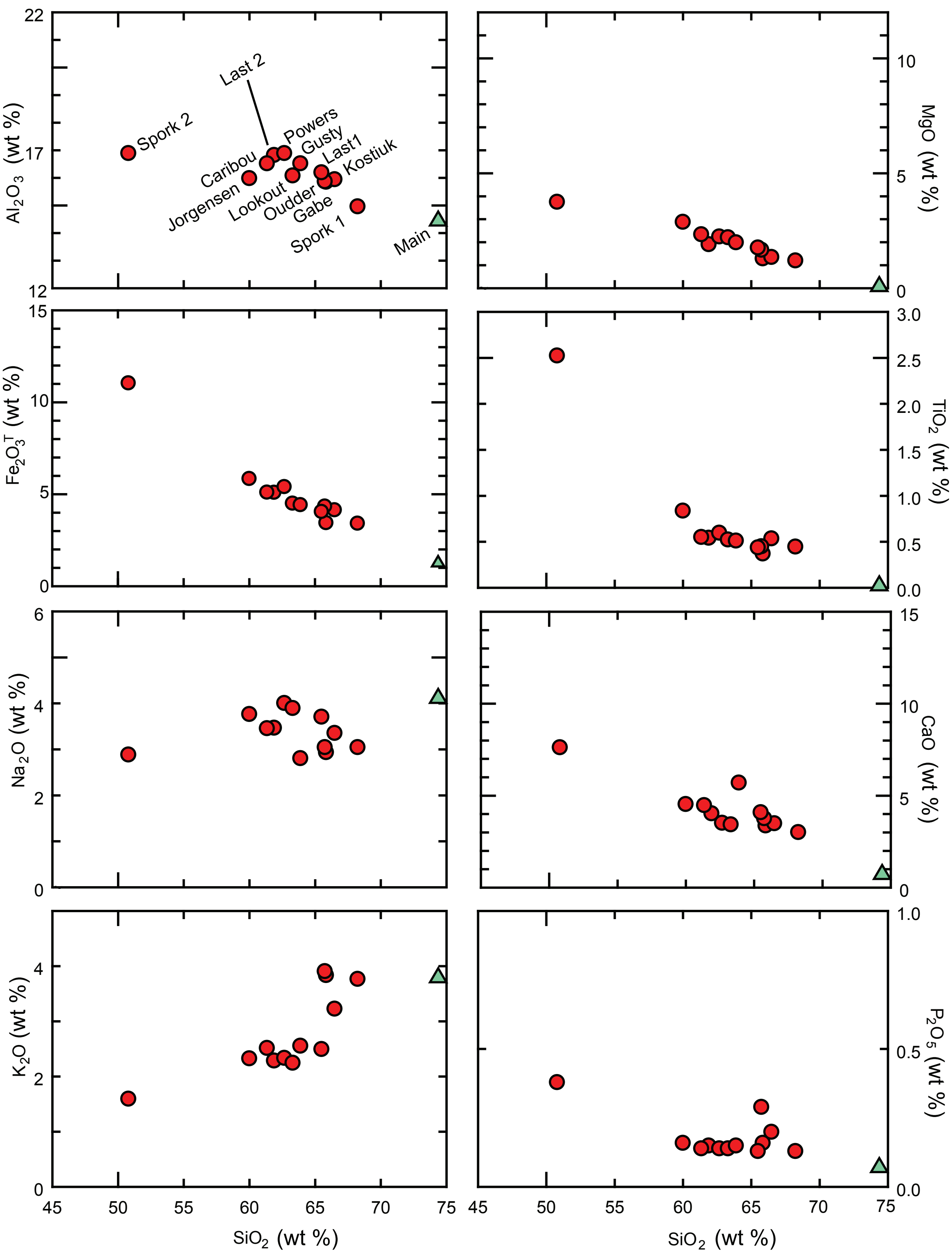

Figure 5. *Major element Harker diagrams for intrusion samples.*

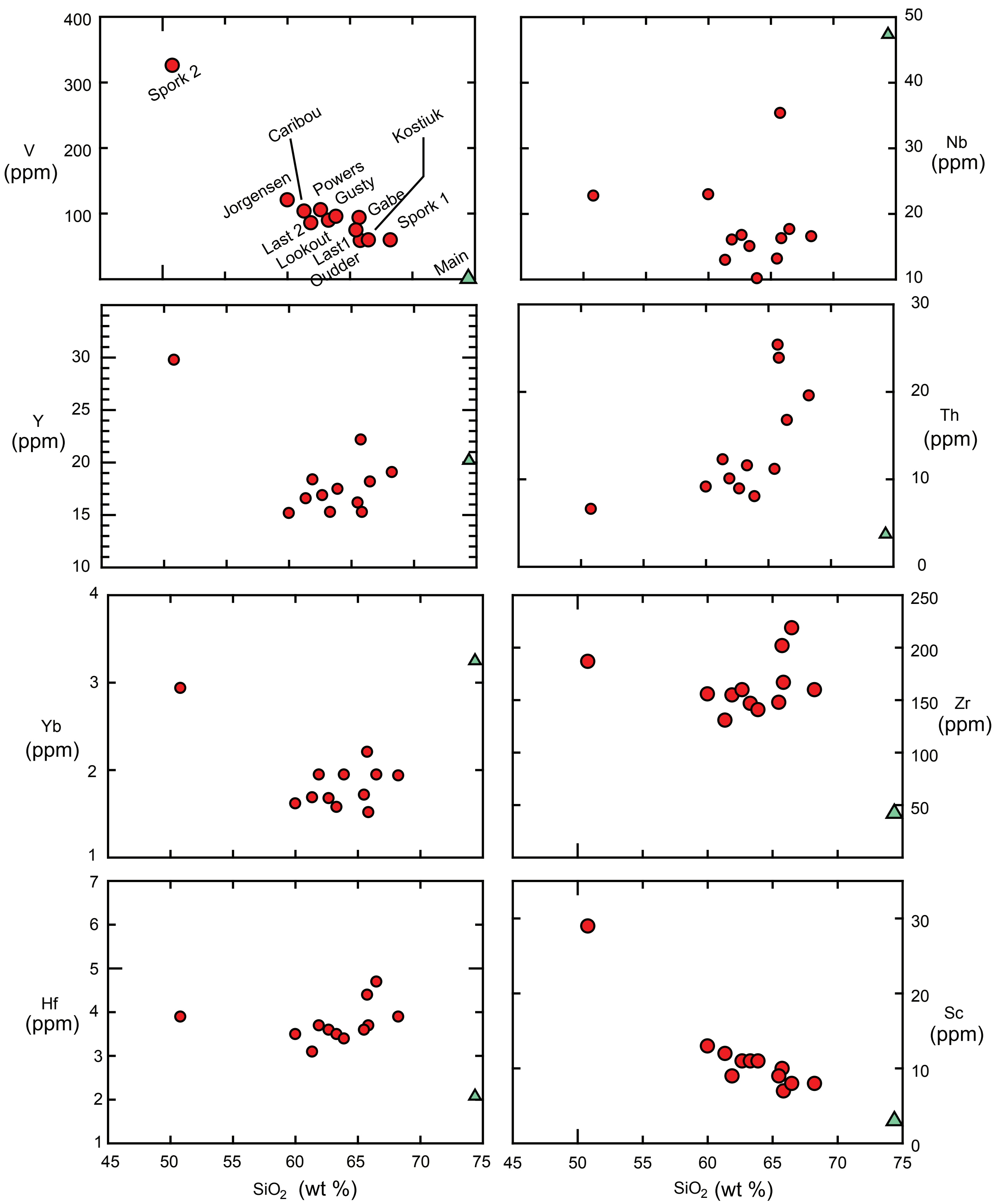

Figure 6. *Harker diagrams for selected trace elements.*

sample is clearly peraluminous. Porphyritic and magnetic samples do not display strong separation in Figure 7. The metaluminous character is fully consistent with modal occurrence of biotite and hornblende as the primary mafic minerals. Most of the samples also straddle the magnetite-ilmenite boundary (Fig. 8); only the sample of the Kostiuk pluton plots clearly within the ilmenite series domain, and Main pluton within the magnetite series domain. For the Kostiuk sample, classification in the ilmenite series is problematic given its very high measured magnetic susceptibility which implies large modal magnetite. No systematic correlation seems to exist between magnetic susceptibility and molar Al content or ferric/ferrous iron ratios. Similarly no apparent relation seems to exist between oxidation ratio in Figure 8 and porphyritic or equigranular texture.

Intrusion compositions normalized to primitive mantle are enriched in all elements except for V and Sc (Fig. 9a). Many of the samples have pronounced depletions in Nb and Ti and a slight depletion in Eu. Intrusion compositions normalized to upper continental crust have element ratios close to 1 (Fig 9b). Elements plotted along the x-axis in both figures are considered immobile under low temperature conditions (Jenner 1996), which is relevant considering the alteration noted in many of the samples. Many of these elements have high field strengths and are incompatible with typical differentiation processes; they are therefore thought to be indicative of their abundance in the source rocks. Normalized concentrations for the Main pluton in Figure 9a,b are significantly different from

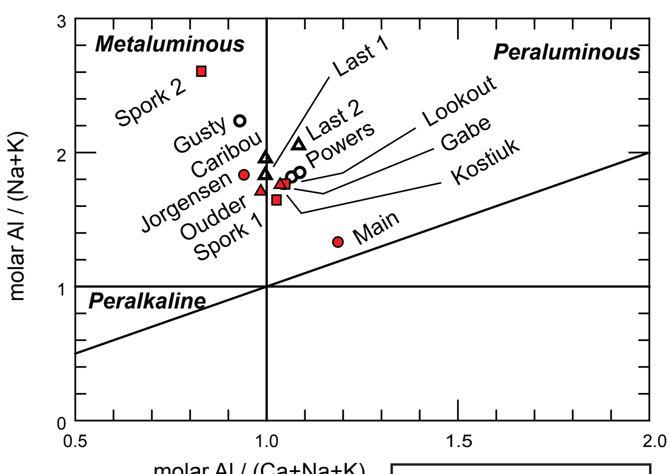

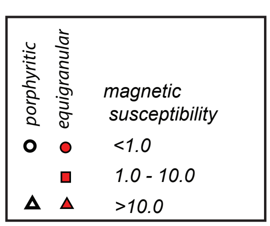

Figure 7. Coal River plutonic samples plotted on Shand index diagram (Manier and Piccoli, 1989).

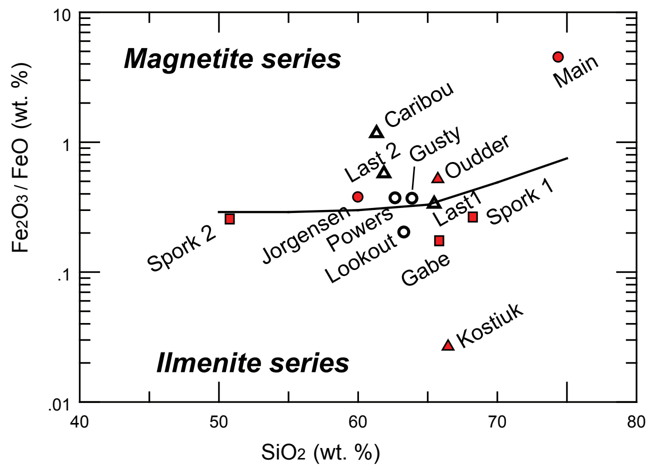

Figure 8. Coal River plutonic samples on magnetite-ilmenite intrusive fields as illustrated in Hart et al. (2004).

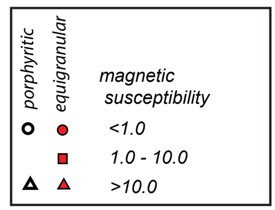

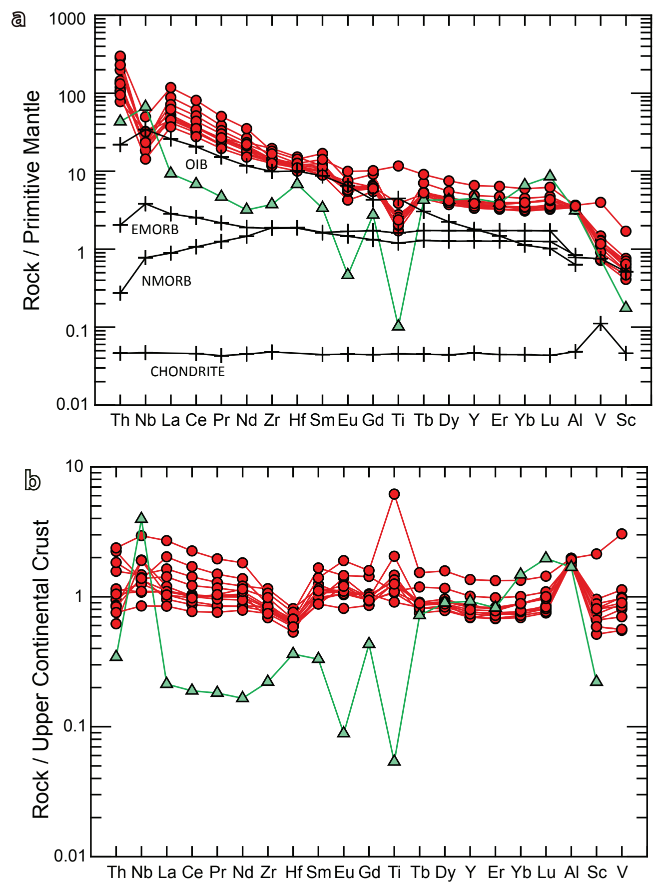

Figure 9. Intrusion compositions normalized to: (a) primitive mantle composition (from Kerrich and Wyman, 1996); (b) upper continental crust composition (from McLennan, 2001). Triangle for sample 10TOA019 (Main intrusion); circles for all other samples.

the other intrusions, raising the possibility that the Main pluton is not part of the same plutonic suite as the other intrusive bodies.

In tectonic discriminant diagrams (Fig. 10a,b,c; Pearce *et al.*, 1984) the intrusions are consistent with syn-collisional (S-type) and volcanic arc (I-type) granite, but the sample from the Main pluton plots in the field for within-plate granite. Most intrusions plot within the volcanic arc or I-type granite (Fig. 10c); however Rb is known to be mobile under many conditions, and the significance of this discriminant is suspect.

In summary, all of the intrusions except for the Main pluton form a chemically coherent plutonic suite. The plutons are generally weakly altered, but immobile elements can be used to determine their chemical affinity. They range from metaluminous to slightly peraluminous, oxidizing to reducing, and plot predominantly within the tectonic discriminant field of volcanic arc-related (or I-type) granites. This chemistry supports the presence of biotite and hornblende as the primary mafic minerals and the general absence of muscovite as a primary mineral. The mineralogy and chemistry of the Main pluton is distinct from the other intrusions. Either it is a more extensively evolved member of this plutonic suite, or it belongs to a different plutonic suite.

U-PB GEOCHRONOLOGY METHODS AND RESULTS

U-Pb ages (Table 2) for nine samples were obtained at Boise State University by the chemical abrasion isotope dilution thermal ionization mass spectrometry (CA ID-TIMS) method from analyses of single zircon grains or fragments of grains following methods described in Pigage *et al.* (2012) as modified from Mattinson (2005). Cathodoluminescent images were used to select zircon grains for dating, based upon zoning patterns and lack of apparent inherited cores (Appendix images A1-A9).

From each sample five or six grains were dated (Table 2; Appendix Figs. A1-A9). Weighted mean $^{206}Pb/^{238}U$ ages for each sample were calculated from equivalent ages using Isoplot 3.0 (Ludwig, 2003) and are interpreted as being the igneous crystallization ages for these plutons. U-Pb dates and uncertainties were calculated using the algorithms of Schmitz and Schoene (2007), $^{235}U/^{205}Pb$ of 77.93 and $^{233}U/^{235}U$ of 1.007066 for the Boise State University tracer solution, and U decay constants recommended by Jaffey *et al.* (1971). $^{206}Pb/^{238}U$ ratios and dates were corrected for initial ^{230}Th disequilibrium using a Th/U[magma]=3

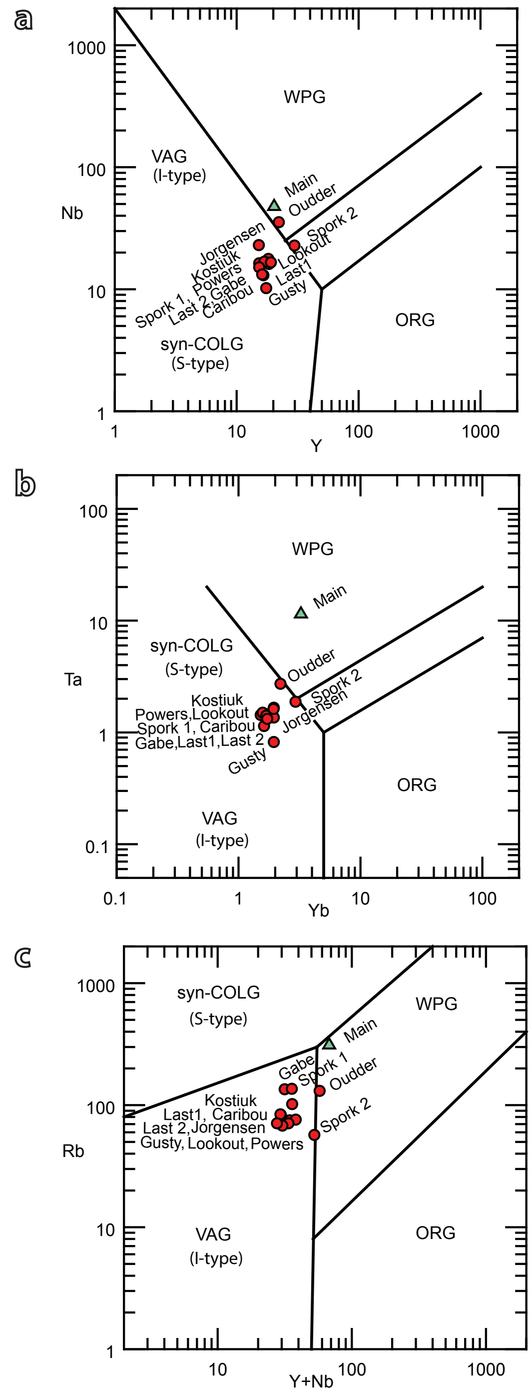

Figure 10. *Tectonic discriminant diagrams for intrusion samples in Coal River map area (from Pearce et al., 1984). Sample 10TOA019 (Main pluton) is indicated by the filled triangle; all other samples indicated with filled circles. (a) Nb vs Y; (b) Ta vs Yb; and (c) Rb vs (Y + Nb); VAG=volcanic arc granite, WPG=within plate granite, COLG=syn-collisional granite, ORG=ocean ridge granite.*

Table 2. *Uranium-lead isotopic CA-TIMS zircon data. Sample locations are in Table 1.*

							Radiogenic Isotope Ratios								Isotopic Dates					
Sample	Th/U	^{206}Pb* x10^{-13} mol	mol % ^{206}Pb*	Pb*/Pb$_c$	Pb$_c$ (pg)	^{206}Pb/^{204}Pb	^{208}Pb/^{206}Pb	^{207}Pb/^{206}Pb	% err	^{207}Pb/^{235}U	% err	^{206}Pb/^{238}U	% err	corr. coef.	^{207}Pb/^{206}Pb	±	^{207}Pb/^{235}U	±	^{206}Pb/^{238}U	±
(a)	(b)	(c)	(c)	(c)	(c)	(d)	(e)	(e)	(f)	(e)	(f)	(e)	(f)		(g)	(f)	(g)	(f)	(g)	(f)
Gusty		Gusty Lake																		
z1	0.252	1.9619	99.85%	193	0.24	12587	0.081	0.048072	0.107	0.103374	0.161	0.015596	0.070	0.863	102.82	2.53	99.89	0.15	99.76	0.07
z2	0.239	0.9393	99.75%	112	0.19	7346	0.076	0.047988	0.185	0.103209	0.229	0.015598	0.073	0.711	98.68	4.38	99.73	0.22	99.78	0.07
z3	0.235	1.1511	99.79%	135	0.20	8851	0.075	0.048014	0.176	0.103257	0.218	0.015597	0.075	0.675	99.98	4.17	99.78	0.21	99.77	0.07
z4	0.229	2.8010	99.86%	207	0.31	13553	0.073	0.048037	0.105	0.103333	0.158	0.015601	0.069	0.863	101.11	2.48	99.85	0.15	99.80	0.07
z5	0.264	1.1166	99.66%	84	0.31	5449	0.084	0.048085	0.220	0.103510	0.260	0.015613	0.073	0.655	103.44	5.19	100.01	0.25	99.87	0.07
z6	0.258	1.8928	99.78%	128	0.34	8342	0.083	0.048526	0.140	0.105236	0.189	0.015729	0.072	0.786	124.99	3.29	101.60	0.18	100.60	0.07
							weighted mean ^{206}Pb/^{238}U date for 5 zircon grains of 99.79 ± 0.03 Ma (MSWD = 1.4)													
Kostiuk		09RAS062																		
z1	0.613	1.6703	99.67%	95	0.45	5604	0.196	0.048010	0.195	0.102842	0.238	0.015536	0.072	0.704	99.76	4.60	99.40	0.23	99.38	0.07
z2	0.655	0.8859	99.45%	57	0.40	3357	0.210	0.048038	0.303	0.102921	0.346	0.015539	0.073	0.646	101.14	7.17	99.47	0.33	99.40	0.07
z3	0.661	1.7171	99.64%	87	0.51	5067	0.211	0.048011	0.213	0.102872	0.254	0.015540	0.072	0.664	99.80	5.03	99.42	0.24	99.41	0.07
z4	0.645	1.2771	99.66%	93	0.35	5473	0.206	0.047989	0.247	0.102786	0.284	0.015534	0.076	0.592	98.71	5.83	99.34	0.27	99.37	0.07
z5	0.639	1.2416	99.29%	44	0.73	2580	0.204	0.048023	0.380	0.102887	0.422	0.015539	0.077	0.613	100.39	8.99	99.44	0.40	99.40	0.08
z6	0.660	0.9236	99.11%	35	0.69	2057	0.211	0.047922	0.472	0.102664	0.518	0.015537	0.075	0.647	95.44	11.18	99.23	0.49	99.39	0.07
							weighted mean ^{206}Pb/^{238}U date for 6 zircon grains of 99.39 ± 0.03 Ma (MSWD = 0.1)													
Last2		09LP098																		
z1	0.340	4.2532	99.84%	178	0.57	11318	0.109	0.048037	0.110	0.102019	0.162	0.015403	0.070	0.838	101.08	2.60	98.64	0.15	98.54	0.07
z3	0.331	2.7269	99.85%	189	0.34	12025	0.106	0.048030	0.107	0.101959	0.160	0.015396	0.069	0.858	100.76	2.53	98.58	0.15	98.49	0.07
z4	0.381	2.6510	99.85%	194	0.33	12183	0.122	0.048073	0.138	0.102118	0.182	0.015406	0.072	0.733	102.88	3.26	98.73	0.17	98.56	0.07
z5	0.350	3.1374	99.84%	183	0.41	11604	0.112	0.048086	0.104	0.102067	0.159	0.015395	0.069	0.869	103.49	2.47	98.68	0.15	98.48	0.07
z6	0.361	2.1651	99.76%	122	0.42	7736	0.116	0.048026	0.142	0.101988	0.189	0.015402	0.070	0.778	100.54	3.35	98.61	0.18	98.53	0.07
							weighted mean ^{206}Pb/^{238}U date for 5 zircon grains of 98.52 ± 0.03 Ma (MSWD = 0.8)													
Jorgensen		09RAS136																		
z1	0.225	1.3220	99.65%	81	0.38	5310	0.072	0.047981	0.199	0.101727	0.242	0.015377	0.070	0.706	98.32	4.70	98.37	0.23	98.37	0.07
z2	0.229	1.6987	99.79%	130	0.30	8538	0.073	0.048015	0.135	0.101783	0.184	0.015374	0.070	0.799	99.99	3.18	98.42	0.17	98.36	0.07
z3	0.244	2.1815	99.83%	161	0.31	10510	0.078	0.048071	0.118	0.101885	0.170	0.015372	0.070	0.843	102.78	2.78	98.51	0.16	98.34	0.07
z4	0.284	0.6361	99.22%	36	0.41	2338	0.091	0.048118	0.438	0.102048	0.485	0.015381	0.082	0.623	105.10	10.35	98.67	0.46	98.40	0.08
z5	0.367	0.6939	99.39%	48	0.35	3021	0.117	0.047938	0.351	0.101547	0.393	0.015363	0.076	0.623	96.21	8.31	98.20	0.37	98.29	0.07
z6	0.289	1.0974	99.28%	39	0.66	2553	0.092	0.048043	0.381	0.101847	0.424	0.015375	0.074	0.627	101.41	9.02	98.48	0.40	98.36	0.07
							weighted mean ^{206}Pb/^{238}U date for 6 zircon grains of 98.35 ± 0.03 Ma (MSWD = 1.0)													
Caribou		09TOA180																		
z1	0.272	3.7709	99.87%	221	0.40	14321	0.087	0.048048	0.097	0.101759	0.152	0.015360	0.069	0.876	101.61	2.29	98.40	0.14	98.27	0.07
z3	0.313	2.3406	99.84%	174	0.32	11133	0.100	0.048077	0.113	0.101861	0.165	0.015366	0.069	0.846	103.04	2.66	98.49	0.15	98.31	0.07
z4	0.351	2.5384	99.61%	74	0.82	4706	0.112	0.048024	0.212	0.101713	0.253	0.015361	0.071	0.674	100.47	5.02	98.36	0.24	98.27	0.07
z5	0.420	2.4326	99.79%	139	0.43	8650	0.134	0.048014	0.134	0.101665	0.182	0.015357	0.071	0.780	99.98	3.17	98.31	0.17	98.24	0.07
z6	0.563	1.9651	99.76%	129	0.38	7744	0.180	0.048032	0.157	0.101699	0.201	0.015356	0.072	0.718	100.85	3.72	98.34	0.19	98.24	0.07
							weighted mean ^{206}Pb/^{238}U date for 5 zircon grains of 98.27 ± 0.03 Ma (MSWD = 0.6)													
Lookout		09TAO179																		
z2	0.393	5.1848	99.91%	336	0.37	21012	0.126	0.048013	0.082	0.101592	0.141	0.015346	0.069	0.917	99.91	1.94	98.24	0.13	98.18	0.07
z3	0.349	4.4313	99.90%	281	0.38	17787	0.112	0.048006	0.093	0.101648	0.148	0.015357	0.070	0.873	99.59	2.20	98.30	0.14	98.24	0.07
z4	0.456	7.1048	99.92%	358	0.49	21766	0.154	0.052448	0.079	0.183004	0.150	0.025306	0.090	0.898	304.98	1.81	170.64	0.24	161.11	0.14
z5	0.393	3.5271	99.71%	102	0.84	6381	0.126	0.048065	0.170	0.101698	0.213	0.015346	0.070	0.710	102.45	4.03	98.34	0.20	98.17	0.07
z6	0.666	4.2218	99.87%	248	0.44	14464	0.213	0.048052	0.085	0.101678	0.145	0.015347	0.069	0.931	101.84	2.01	98.32	0.14	98.18	0.07
z7	0.381	4.0498	99.88%	253	0.39	15877	0.122	0.048026	0.092	0.101669	0.148	0.015354	0.070	0.889	100.53	2.17	98.32	0.14	98.22	0.07
							weighted mean ^{206}Pb/^{238}U date for 5 zircon grains of 98.20 ± 0.03 Ma (MSWD = 0.9)													

Table 2. *continued.*

Sample	Th/U	$^{206}Pb^*$ x10^{-13} mol	mol % $^{206}Pb^*$	Pb^*/Pb_c	Pb$_c$ (pg)	$^{206}Pb/^{204}Pb$	Radiogenic Isotope Ratios: $^{208}Pb/^{206}Pb$	$^{207}Pb/^{206}Pb$	% err	$^{207}Pb/^{235}U$	% err	$^{206}Pb/^{238}U$	% err	corr. coef.	Isotopic Dates: $^{207}Pb/^{206}Pb$	±	$^{207}Pb/^{235}U$	±	$^{206}Pb/^{238}U$	±
(a)	(b)	(c)	(c)	(c)	(c)	(d)	(e)	(e)	(f)	(e)	(f)	(e)	(f)		(g)	(f)	(g)	(f)	(g)	(f)
Spork1		10TOA014																		
z1	0.462	6.0370	99.95%	656	0.23	40238	0.148	0.048020	0.070	0.101516	0.133	0.015332	0.070	0.951	100.28	1.65	98.18	0.12	98.09	0.07
z2	0.452	1.9876	99.85%	201	0.24	12397	0.145	0.048038	0.128	0.101513	0.176	0.015326	0.071	0.787	101.16	3.03	98.17	0.17	98.05	0.07
z3	0.504	2.2253	99.90%	289	0.19	17547	0.161	0.048041	0.096	0.101521	0.151	0.015326	0.070	0.877	101.31	2.27	98.18	0.14	98.05	0.07
z4	0.417	3.6900	99.90%	294	0.31	18288	0.134	0.048033	0.089	0.101581	0.147	0.015338	0.071	0.897	100.90	2.10	98.23	0.14	98.12	0.07
z5	0.458	3.3013	99.91%	346	0.24	21246	0.147	0.048044	0.102	0.101606	0.154	0.015338	0.070	0.841	101.43	2.41	98.26	0.14	98.13	0.07
z6	0.577	2.3570	99.84%	197	0.30	11751	0.185	0.047974	0.112	0.101418	0.164	0.015332	0.069	0.840	97.98	2.66	98.08	0.15	98.09	0.07
weighted mean $^{206}Pb/^{238}U$ date for 6 zircon grains of 98.09 ± 0.03 Ma (MSWD = 1.0)																				
Gabe		09LP048																		
z1	0.236	6.4116	99.95%	517	0.29	33773	0.076	0.048039	0.072	0.101323	0.134	0.015297	0.070	0.939	101.21	1.71	98.00	0.13	97.87	0.07
z2	0.233	9.4835	99.83%	167	1.31	10987	0.075	0.048070	0.096	0.101365	0.151	0.015294	0.072	0.871	102.69	2.26	98.04	0.14	97.84	0.07
z3	0.284	3.6880	99.87%	215	0.40	13893	0.091	0.047990	0.103	0.101206	0.156	0.015295	0.070	0.855	98.77	2.44	97.89	0.15	97.85	0.07
z4	0.210	4.5338	99.87%	217	0.48	14312	0.067	0.048049	0.093	0.101280	0.149	0.015288	0.070	0.885	101.66	2.21	97.96	0.14	97.80	0.07
z5	0.252	4.4302	99.89%	253	0.41	16503	0.081	0.048001	0.095	0.101174	0.150	0.015287	0.070	0.869	99.33	2.26	97.86	0.14	97.80	0.07
z6	0.200	6.9512	99.89%	261	0.61	17272	0.064	0.048049	0.087	0.101280	0.145	0.015288	0.072	0.891	101.67	2.07	97.96	0.14	97.80	0.07
weighted mean $^{206}Pb/^{238}U$ date for 6 zircon grains of 97.83 ± 0.03 Ma (MSWD = 0.7)																				
Oudder		09TOA135																		
z1	0.448	11.5824	99.95%	638	0.45	39298	0.144	0.048018	0.068	0.101138	0.131	0.015276	0.071	0.950	100.13	1.60	97.83	0.12	97.73	0.07
z2	0.406	5.0870	99.90%	307	0.40	19168	0.130	0.048038	0.078	0.101181	0.138	0.015276	0.069	0.933	101.13	1.84	97.87	0.13	97.73	0.07
z3	0.303	4.7393	99.89%	268	0.42	17201	0.097	0.048019	0.083	0.101129	0.142	0.015274	0.069	0.916	100.22	1.97	97.82	0.13	97.72	0.07
z4	0.353	2.6732	99.82%	164	0.39	10408	0.113	0.048030	0.114	0.101101	0.166	0.015267	0.069	0.841	100.74	2.70	97.79	0.15	97.67	0.07
z5	0.357	2.5063	99.63%	79	0.76	5016	0.115	0.048058	0.210	0.101154	0.251	0.015266	0.071	0.667	102.10	4.97	97.84	0.23	97.67	0.07
z6	0.327	2.2775	99.73%	106	0.51	6759	0.105	0.048067	0.158	0.101213	0.203	0.015272	0.070	0.745	102.58	3.74	97.90	0.19	97.70	0.07
weighted mean $^{206}Pb/^{238}U$ date for 6 zircon grains of 97.70 ± 0.03 Ma (MSWD = 0.7)																				

(a) z1, z2, *etc.* are labels for analyses composed of single zircon grains that were annealed and chemically abraded (Mattinson, 2005). Fraction labels in bold denote analyses used in the weighted mean calculations.

(b) Model Th/U ratio calculated from radiogenic $^{208}Pb/^{206}Pb$ ratio and $^{207}Pb/^{235}U$ date.

(c) Pb* and Pbc are radiogenic and common Pb, respectively. mol % $^{206}Pb^*$ is with respect to radiogenic and blank Pb.

(d) Measured ratio corrected for spike and fractionation only. Fractionation correction is 0.15 ± 0.03 (1 sigma) %/amu (atomic mass unit) for single-collector Daly analyses, based on analysis of EARTHTIME 202Pb-205Pb tracer solution.

(e) Corrected for fractionation, spike, common Pb, and initial disequilibrium in $^{230}Th/^{238}U$. Common Pb is assigned to procedural blank with composition of $^{206}Pb/^{204}Pb$ = 18.35 ± 1.50%; $^{207}Pb/^{204}Pb$ = 15.60 ± 0.75%; $^{208}Pb/^{204}Pb$ = 38.08 ± 1.00% (1 sigma). $^{206}Pb/^{238}U$ and $^{207}Pb/^{206}Pb$ ratios corrected for initial disequilibrium in $^{230}Th/^{238}U$ using Th/U [magma] = 3.

(f) Errors are 2 sigma, propagated using algorithms of Schmitz and Schoene (2007) and Crowley *et al.* (2007).

(g) Calculations based on the decay constants of Jaffey *et al.* (1971). $^{206}Pb/^{238}U$ and $^{207}Pb/^{206}Pb$ dates corrected for initial disequilibrium in $^{230}Th/^{238}U$ using Th/U [magma] = 3.

using the algorithms of Crowley *et al.* (2007), resulting in an increase in the $^{206}Pb/^{238}U$ dates of ~0.09 Ma. All common Pb in analyses was attributed to laboratory blank and subtracted based on the measured laboratory Pb isotopic composition and associated uncertainty. U blanks are difficult to precisely measure, but are estimated at 0.07 pg.

Errors are the internal errors given at the 2 sigma confidence interval based on analytical uncertainties only, including counting statistics, subtraction of tracer solution, and blank and initial common Pb subtraction. These errors should be considered when comparing our dates with $^{206}Pb/^{238}U$ dates from other laboratories that used the same Boise State University tracer solution or a tracer solution that was cross-calibrated using EARTHTIME gravimetric standards. When comparing our dates with those derived from other geochronological methods using the U-Pb decay scheme (*e.g.*, laser ablation ICP-MS), a systematic uncertainty in the tracer calibration should be added to the internal error in quadrature; this error is ±0.10 Ma for all samples, resulting in a 2 sigma error of ±0.13 Ma. When comparing our dates with those derived from other decay schemes (*e.g.*, $^{40}Ar/^{39}Ar$, $^{187}Re^{187}Os$), systematic uncertainties in the tracer calibration and ^{238}U decay constant (Jaffey *et al.*, 1971) should be added to the internal error in quadrature. This error is ± 0.15 Ma for all samples, resulting in a combined 2 sigma error of ±0.18 Ma.

The $^{206}Pb/^{238}U$ weighted mean ages for zircon grains from the nine plutons range from 99.79±0.03 Ma to 97.70±0.03 Ma (Fig. 11). One zircon grain from the Gusty Lake sample (grain z6, Table 2) yielded an older date of 100.60±0.07 Ma and it was not used in calculating the weighted mean. Also, one grain from the Lookout sample (grain z4; Table 2) that yielded an older, discordant date of 161 Ma (Table 2) was not used in the calculation of the weighted mean date. Unfortunately the sample from the Main stock (sample10TOA019) yielded such poor quality zircon that isotopic dating was not attempted. The agreement of the high-precision single-grain dates within each sample and the simple CL zoning patterns (*cf.* Appendix) indicate this range reflects the timing of intrusion rather than Pb loss or inheritance.

The age range of nine plutons spread across a 100 x 30 km area is only 2.1 Ma. No systematic change in age across the map is apparent (Fig. 3). The three plutons (Jorgensen, Caribou, Lookout) in the northeast corner of the map area have an age spread of less than 0.1 Ma.

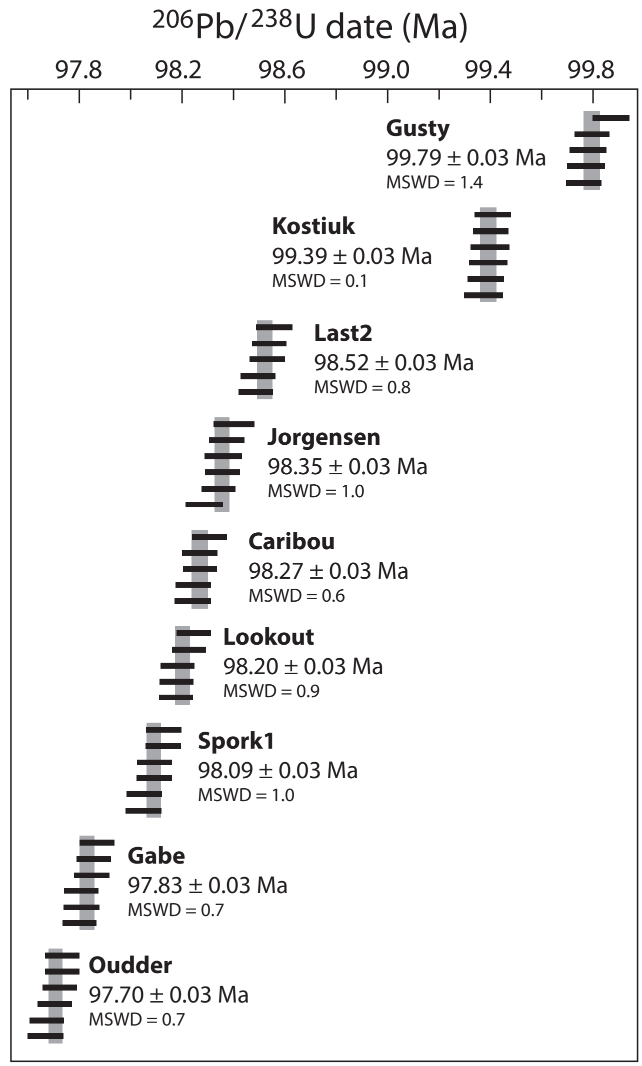

Figure 11. *Plot of new $^{206}Pb/^{238}U$ dates from single zircon grains from plutons in Coal River map area. Plotted with Isoplot 3.0 (Ludwig, 2003). Solid horizontal bars are 2 sigma internal errors. Weighted mean date is represented by the grey box behind the error bars.*

DISCUSSION

Our geochronological results are comparable to those completed by Heffernan (2004), Rasmussen *et al.* (2007), and Rasmussen (2013) in the region. Previous U-Pb ID-TIMS dating of the Patterson pluton (Fig. 3) used a single, abraded fraction of poor to moderate quality zircon to interpret an age of 97.5±0.5 Ma (Heffernan, 2004). Discordant dates from other fractions were deemed the result of inheritance. ID-TIMS dating of two fractions of monazite from a felsic dyke near the Patterson pluton yielded an age of 98.3±1.6 Ma (Heffernan, 2004). These relatively imprecise dates complement ages from the same area reported here. U-Pb dating of zircon from the Powers pluton by the laser ablation inductively coupled plasma mass spectrometry (LA-ICP-MS) method yielded an age of 98.2 ± 1.3 Ma (Rasmussen *et al.*, 2007). This date is similar to those from the same area reported here. U-Pb dating of zircon from the Jorgensen pluton by Rasmussen *et al.* (2007, sample KR-05-08, mistakenly listed in their Table 2 as the Powers pluton) yielded an age of 102.4 ± 2.3 Ma; a more recent re-analysis of this sample resulted in an age of 95.9 ± 0.8 Ma (Rasmussen, 2013). ^{40}Ar ^{39}Ar dating of biotite from this sample yielded an age of 101.4 ± 0.6 Ma (Rasmussen *et al.*, 2007). These ages do not agree with the age of 98.35 ± 0.03 Ma from the Jorgensen pluton reported here, which is a robust age based on six high-precision CA-TIMS ages.

With the exception of the undated Main pluton, the similar chemistry and crystallization ages for all plutons dated in this study indicate they constitute a single plutonic suite. The compositions, mineralogy and crystallization ages of the dated Coal River intrusions support their logical inclusion in the Tay River plutonic suite as defined by Mortensen *et al.* (2000) and discussed further by Heffernan (2004), Rasmussen *et al.* (2007), and Rasmussen (2013).

Heffernan (2004) and Rasmussen *et al.* (2007) reported whole rock geochemistry for the Patterson, Jorgensen and Power plutons. Trace element plots normalized to primitive mantle for their samples fall within the envelope of plutonic samples reported in this study. High initial $^{87}Sr/^{86}Sr$ and epsilon Nd (εNd) values (Heffernan, 2004) and ^{18}O signatures (Rasmussen and Arehart, 2010) for these samples are consistent with the parental melts for the intrusions being sourced primarily, if not completely, from crustal rocks. Our element plots normalized to upper continental crust (Fig. 9b) are fully consistent with the sampled intrusions arising from partial melting of continental crust.

The overall limited geochemical variation in the granitoid samples implies a homogenous source material for the intrusions. Trends shown by the Harker diagrams reflect a liquid line of descent from a single magmatic source, with the possible exception of the Main pluton. The petrology of the samples, their metaluminous character and distribution on the tectonic discriminant diagrams further imply that the intrusions correlate best with I-type granites. For similar reasons Rasmussen (2013) considered these intrusions to be sourced from a homogenous, infracrustal source.

Immediately north of the Coal River map area coeval Tay River suite intrusions (including the Mount Kostiuk pluton, Coal River batholith, Spork pluton, and Ivo-Salivo pluton) are more extensively exposed, and not circular in plan (Heffernan, 2004; Rasmussen *et al.*, 2007; Fig. 12).

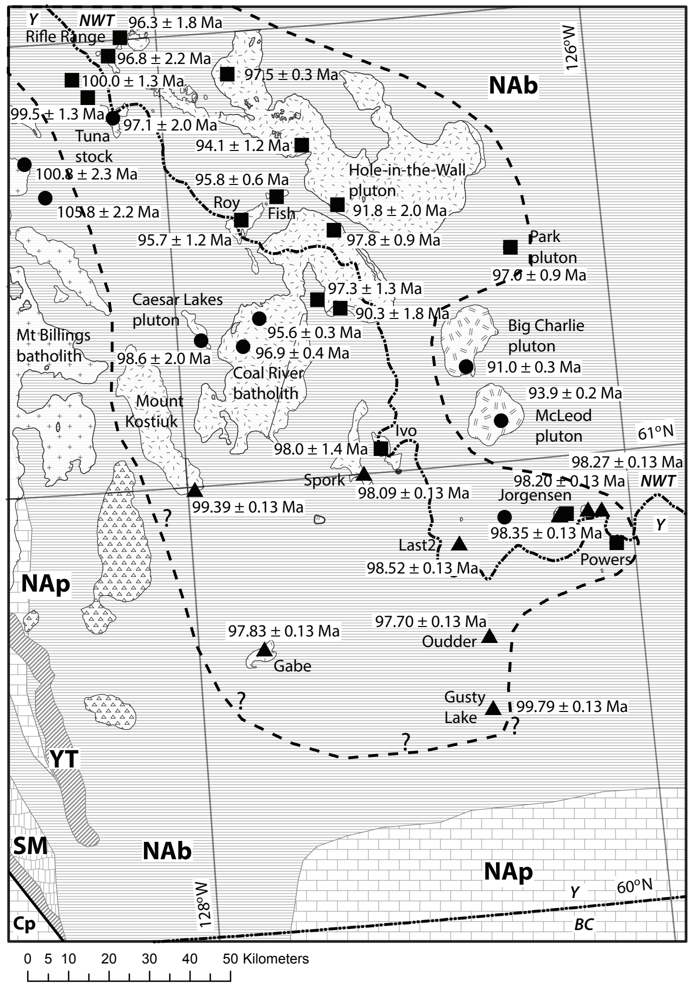

Figure 12. Cretaceous intrusions in southeast Yukon and southwest Northwest Territories superimposed on the distribution of terranes and igneous bodies (from Colpron and Nelson, 2011; Gordey and Makepeace, 2003). Filled circles are ages from Heffernan (2004); filled squares are ages from Rasmussen et al. (2007); filled triangles are ages reported here. Error limits on ages from this paper are ±2 sigma, including analytical error and uncertainty in the tracer calibration. Large plutons of the Anvil suite indicated by the cross pattern; Tay River plutonic suite denoted with random single line pattern (and encircled by the heavy dashed line); Tombstone plutonic suite indicated with random double line pattern; intrusions with unknown affiliation indicated with triangle pattern. NAb: basinal strata of North America; NAp: platformal strata of North America; Y: Yukon; NWT: Northwest Territories, BC: British Columbia.

Crystallization ages for these intrusions are similar or slightly younger than the ages in our study area (Heffernan, 2004; Rasmussen *et al.*, 2007; Rasmussen, 2013). This apparent exposure difference has an approximate easterly orientation and appears to define the gradational southern edge of Tay River suite intrusions in Yukon. No apparent fault or plunging fold structures have been mapped to indicate that the transition from large, irregular to small, circular plan view exposures might be related to exposure of different structural levels.

The intrusions are almost entirely unfoliated (in a few localities incipiently foliated), indicating late syntectonic to post-tectonic crystallization. The interpreted map pattern for the slightly foliated Gabe intrusion suggests that intrusion post-dated significant offset on the reverse, normal and strike-slip faults traced into the area (Pigage *et al.*, 2011). Regional fabric-forming deformation at the exposed structural level therefore ceased before *ca.* 98 Ma.

Plutons of the 99-95 Ma Tay River suite occur in a 70-150 km wide belt that extends ~465 km northwest from the Coal River area in southeast Yukon to northwest of Faro (Mortensen *et al.*, 2000; Rasmussen, 2013). This belt is a subset of an arcuate belt of plutons of early and mid-Cretaceous age (Woodsworth *et al.*, 1991; Mortensen *et al.*, 1995; 2000; Hart *et al.*, 2004; Rasmussen, 2013) on the northeast side of Tintina fault (Fig. 13). When the 430 km of dextral offset is restored (Gabrielse *et al.*, 2006), the aggregate plutonic belt extends westward to include the Livengood and Fairbanks-Salcha suites in central Alaska, and southward to link with coeval plutons in the Pelly and Cassiar mountains of south-central Yukon and adjacent British Columbia.

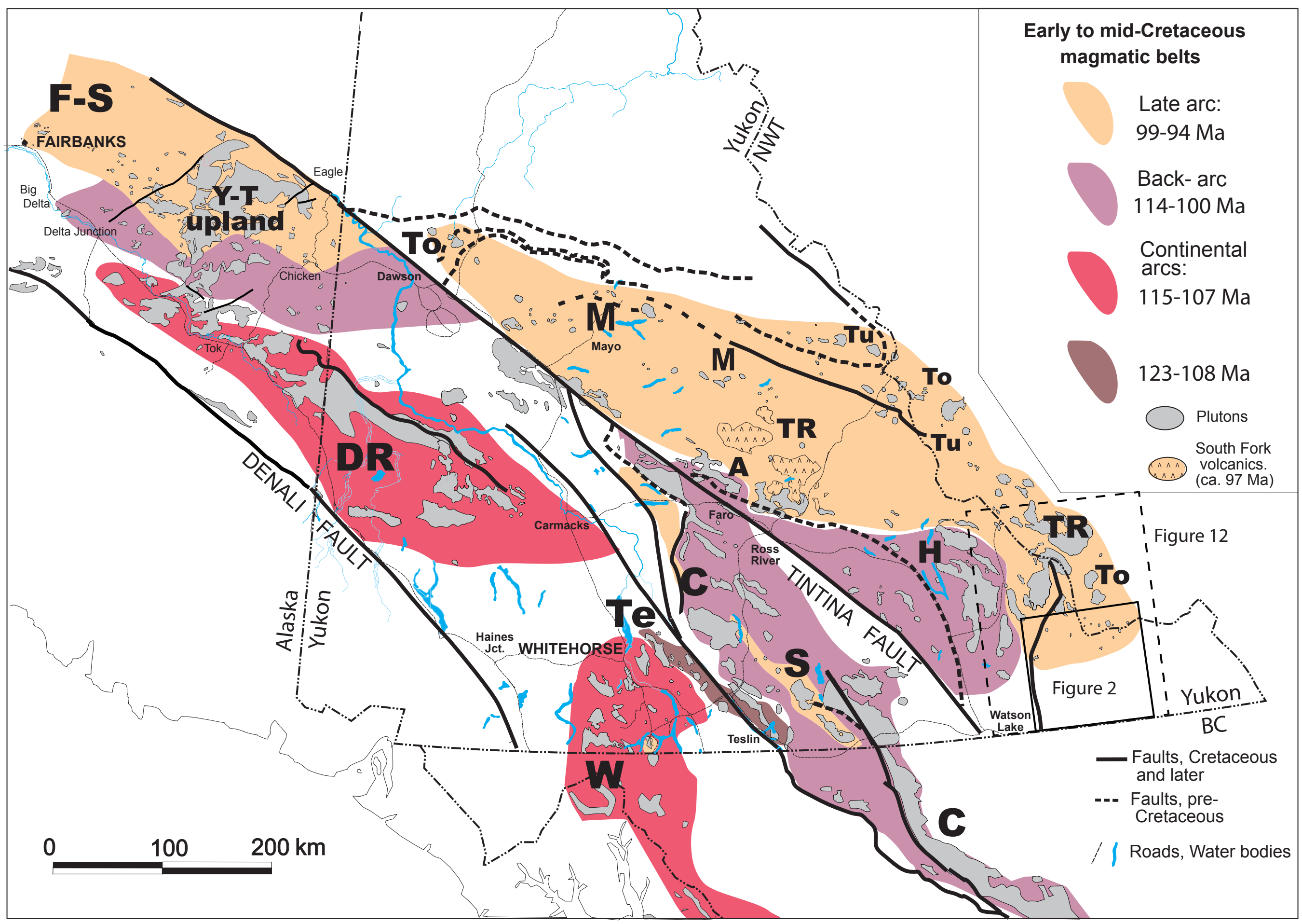

Figure 13. *Distribution of Early to mid-Cretaceous plutons and volcanic rocks (from Hart et al., 2004a) and their generalized magmatic belts reflecting geochronology by Rasmussen (2013), Heffernan (2004) and Mortensen et al. (2000). The approximate locations of plutonic suites are labeled: A = Anvil, C = Cassiar, DR = Dawson Range, F–S = Fairbanks–Salcha, H = Hyland, M = Mayo, S = Seagull–Thirtymile, Te = Teslin, To = Tombstone, TR = Tay River, Tu = Tungsten, W = Whitehorse, and Y-T upland = Yukon–Tanana Upland (modified from Rasmussen, 2013; Figure 1.4a).*

The composition and isotopic systematics of the late Early Cretaceous plutons are consistent with an arc setting, and the concept of a continental arc and inboard back-arc is widely accepted (*e.g.*, Woodsworth *et al.*, 1991; Mortensen *et al.*, 1995, 2000; Hart *et al.*, 2004; Rasmussen, 2013). They are interpreted to be the product of northeastward subduction of the Gravina ocean crust beneath the northwestward drifting North America continent in Early and mid-Cretaceous time (Engebretson *et al.*, 1985; Nelson *et al.*, 2013). Magmatism peaked within the northern Cordillera between 115 to 100 Ma with the voluminous intrusion of the Whitehorse-Coffee Creek suite (arc), and the Cassiar, Anvil and Hyland suites (back-arc; Hart *et al.*, 2004; Rasmussen, 2013).

Following Early to mid-Cretaceous arc and back-arc plutonism, mid-Cretaceous magmatism northeast of Tintina Trench resulted in successive broadly northwest-trending belts of plutons constituting the Tay River (99-96 Ma), Tungsten (98-95 Ma), Mayo (98-93 Ma), and Tombstone (94-89 Ma) plutonic suites and South Fork volcanism (112-93.7 Ma; Table 5a in Gordey, in press). All of the suites form convex bands extending easterly from the Tintina fault and curving to a more southerly trend near the Yukon-NWT border (Fig. 13). All are east (farther inboard) of the earlier Anvil and Hyland suite back-arc intrusions. The locus of plutonism moved east and north with progressively younger plutonic suites (Rasmussen, 2013). Geochemistry comparison (Rasmussen, 2013) of the different suites suggests that all but the Tungsten suite are I-type and formed as partial melts of infracrustal igneous source rocks. In contrast the Tungsten suite has been identified as a mixed suite with both S-type and I-type affinity, depending on location.

The arc magmatism interpretation for these mid-Cretaceous plutonic suite belts is problematic in that the northeast-facing subduction zone would have been located at least 400 km southwest (outboard) of the present location of the plutons. Rasmussen (2013) suggested that the occurrence of I-type magmatism hundreds of kilometres northeast (inboard) from the subduction trench may have been related to flattening of the subducting slab, moving the zone of mantle hydration farther inland. Higher heat flow leading to magma genesis could have been related to mantle convection around the descending slab, although slab break-off is unlikely or possibly occurred later (as indicated by the relative inhomogeneity of the Tombstone and Tungsten suites).

The termination in a southward direction of the Tay River suite plutons in the Coal River map area suggests that the geometry of the subducting slab changed southward, resulting in displacement or cessation of arc magmatism along strike to the south.

CONCLUSIONS

Intrusions in the Coal River map area of southeastern Yukon are predominantly equigranular or porphyritic, biotite ± hornblende granodiorite with lesser tonalite, granite quartz monzodiorite and quartz diorite. They are characterized by a range of magnetic susceptibilities from 0.0 to 17.8 (10^{-3} SI units), consistent major and trace element compositions corresponding to magnetite to ilmenite series intrusions and largely metaluminous to slightly peraluminous affinities. Their whole rock geochemical character and age suggests that they belong to the Tay River plutonic suite (except for the Main pluton) which was sourced from partial melting of a homogenous, infracrustal, igneous parent.

Most of the intrusions are approximately subcircular with steep to vertical intrusive contacts. Regional aeromagnetic surveys were helpful for locating intrusions in areas of poor bedrock exposure.

U-Pb CA ID-TIMS zircon crystallization ages from nine plutons range from 99.79 ± 0.03 to 97.70 ± 0.03 Ma, a spread of only 2.1 Ma. The plutons are late syntectonic to post-tectonic, putting an upper age restriction on deformation of the Cordilleran orogeny in the Coal River area at the exposed structural level.

The Tay River plutonic suite in Yukon and Northwest Territories is part of a northwest-trending belt of relatively homogeneous plutons that represent an intermediate phase (in both location and time) of the continental arc response to subduction and accretion along the Cordilleran margin.

ACKNOWLEDGEMENTS

This project was initiated under the Geoscience for Energy and Minerals (GEM) program of the Geological Survey of Canada and was continued by the Yukon Geological Survey. Field assistants Martina Bezzola, Casey Cardinal, Gavin Clarkson, Kristy Long, and Sarah Shoniker were uncomplaining in a surprisingly vegetated field area. Helicopter assistance was provided by HeliDynamics Ltd. (2009) and Trans North Helicopters (2010). Beth Hunt kept everyone well fed during the 2009 fieldwork. Geochronology in both years was funded by Geological

Survey of Canada. Michael Burns and Bev Quist of McEvoy Geosciences Ltd. kindly collected a granitic sample from near Gusty Lake.

This manuscript is a joint Yukon Geological Survey and Earth Sciences Sector (20120369) contribution. David Moynihan (Yukon Geological Survey) and Bob Anderson (Geological Survey of Canada) improved an earlier version, and we also thank reviewer Don Murphy and editor Patrick Sack.

REFERENCES

Cecile, M.P., Morrow, D.W., and Williams, G.K., 1997. Early Paleozoic (Cambrian to Early Devonian) tectonic framework, Canadian Cordillera. Bulletin of Canadian Petroleum Geology, vol. 45, p. 54-74.

Colpron, M. and Nelson, J.L., 2011. A digital atlas of terranes for the Northern Cordillera. Accessed online from: Yukon Geological Survey <*www.geology.gov.yk.ca*> [accessed July 15, 2012].

Crowley, J.L., Schoene, B., and Bowring, S.A., 2007. U-Pb dating of zircon in the Bishop Tuff at the millennial scale: Geology, vol. 35, p. 1123-1126.

Engebretson, D.C., Cox, A., and Gordon, R.G., 1985. Relative motions between oceanic and continental plates in the Pacific basin. Geological Society of America, Special Paper 206, 59 p.

Frost, B.R., Barnes, C.G., Collins, W.J., Arculus, R.J., Ellis, D.J., and Frost, C.D., 2001. A geochemical classification for granitic rocks. Journal of Petrology, vol. 42, p. 2033-2048.

Gabrielse, H. and Blusson, S., 1969. Geology of Coal River map-area, Yukon Territory and District of Mackenzie (95D). Geological Survey of Canada, Paper 68-38, 22 p.

Gabrielse H., 1973. Geology of Flat River, Glacier Lake and Wrigley Map-Areas, District of Mackenzie and Yukon Territory. Geological Survey of Canada, Memoir 366, Part I, 153 p.

Gabrielse, H., Murphy, D.C., and Mortensen, J.K., 2006. Cretaceous and Cenozoic dextral orogeny-parallel, displacements, magmatism, and paleogeography, north-central Canadian Cordillera. *In:* Paleogeography of the North American Cordillera: Evidence for and against large-scale displacements. J.W. Haggart, R.J. Enkin, and J.W.H. Monger (eds.), Geological Association of Canada, Special Paper 46, p. 255-276.

Gordey, S.P., 1988. The South Fork volcanics: mid-Cretaceous caldera fill tuffs in east central Yukon. *In:* Current Research, part E: Cordillera and Pacific margin, Geological Survey of Canada, Paper no. 88-1E, p. 13-18.

Gordey, S.P., in press. Evolution of the Selwyn basin region, Sheldon Lake (105J) and Tay River (105K) map areas, central Yukon Territory. Geological Survey of Canada, Bulletin 599, 274 p.

Gordey, S.P. and Anderson, R.J., 1993. Evolution of the northern Cordilleran miogeocline, Nahanni map area (105I), Yukon and Northwest Territories. Geological Survey of Canada, Memoir 428, 214 p.

Gordey, S.P. and Makepeace, A.J., 2003. Yukon digital geology, version 2.0. Geological Survey of Canada, Open File 1749 and Yukon Geological Survey, Open File 2003-9 (D), 2 CD-ROMs.

Hart, C.J.R., Goldfarb, R.J., Lewis, L.L., and Mair, J.L., 2004. The Northern Cordilleran mid-Cretaceous plutonic province: Ilmenite/Magnetite-series granitoids and intrusion-related mineralization. Resource Geology, vol. 54, p. 253-280.

Heffernan, R.S., 2004. Temporal, geochemical, isotopic, and metallogenic studies of mid-Cretaceous magmatism in the Tintina Gold Province, southeastern Yukon and southwestern Northwest Territories, Canada. Unpublished MSc thesis, University of British Columbia, 83 p.

Jaffey, A.H., Flynn, K.F., Glendenin, L.E., Bentley, W.C., and Essling, A.M., 1971. Precision measurements of half-lives and specific activities of ^{235}U and ^{238}U. Physical Review C, vol. 4, p. 1889-1906.

Jenner, G.A., 1996. Trace element geochemistry of igneous rocks: geochemical nomenclature and analytical geochemistry. *In:* Trace Element Geochemistry of Volcanic Rocks: Applications for massive sulphide exploration, D.A. Wyman (ed.), Geological Association of Canada, Short Course Notes, vol. 12, p. 51-77.

Kerrich, R. and Wyman, D.A., 1996. The trace element systematics of igneous rocks in mineral exploration: an overview. *In:* Trace Element Geochemistry of Volcanic Rocks: Applications for massive sulphide exploration. D.A. Wyman (ed.), Geological Association of Canada, Short Course Notes, vol. 12, p. 1-50.

Long, D.F. and Sweet, A.F., 1994. Age and depositional environment of the Rock River coal basin, Yukon Territory, Canada. Canadian Journal Earth Sciences, vol. 31, p. 865-880.

Ludwig, K.R., 2003. User's Manual for Isoplot 3.00. Berkeley Geochronology Center: Berkeley, CA.

Mair, J.L., Hart, C.R.J., and Stephens, J.R., 2006. Deformation history of the northwestern Selwyn Basin, Yukon, Canada: implications for orogeny evolution and mid-Cretaceous magmatism. Bulletin of Geological Society of America, vol. 118, p. 304-323.

Maniar, P.D. and Piccoli, P.M., 1989. Tectonic discrimination of granitoids. Bulletin of Geological Society of America, vol. 101, p. 635-643.

Mattinson, J.M., 2005. Zircon U-Pb chemical abrasion ("CA-TIMS") method: combined annealing and multi-step partial dissolution analysis for improved precision and accuracy of zircon ages. Chemical Geology, vol. 220, p. 47-66.

McLennan, S.M., 2001. Relationships between the trace element composition of sedimentary rocks and upper continental crust. Geochemistry, Geophysics, Geosystems, vol. 2, p. 1021.

Mortensen, J.K., Hart, C.J.R., Murphy, D.C., and Heffernan, S., 2000. Temporal evolution of early and mid-Cretaceous magmatism in the Tintina Gold Belt. *In:* The Tintina Gold Belt: Concepts, Exploration, and Discoveries. T. Tucker and M.T. Smith (eds.). British Columbia and Yukon Chamber of Mines, Special Volume 2, p. 49-58.

Mortensen, J.K., Murphy, D.C., Hart, C.J.R., and Anderson, R.G., 1995. Timing, tectonic setting, and metallogeny of Early and mid-Cretaceous magmatism in Yukon Territory. Geological Society of America Program Abstracts, vol. 27, p. 65.

Natural Resources Canada, 2009. Canadian Aeromagnetic Data Base, Geoscience Data Repository; Geological Survey of Canada, <*http://gdrdap.agg.nrcan.gc.ca/geodap/home/Default.aspx?lang=e*> [accessed April 1, 2009]

Nelson, J. and Colpron, M., 2007. Tectonics and metallogeny of the British Columbia, Yukon and Alaskan Cordillera, 1.8 Ga to the present. *In:* Mineral Deposits of Canada: A synthesis of major deposit-types, district metallogeny, the evolution of geological provinces, and exploration methods, W.D. Goodfellow (ed.), Geological Association of Canada, Mineral Deposits Division, Special Publication No. 5, p. 755-791.

Nelson, J.L., Colpron, M., and Israel, S., 2013. The Cordillera of British Columbia, Yukon, and Alaska: Tectonics and Metallogeny. *In:* Tectonics, Metallogeny, and Discovery: The North American Cordillera and Similar Accretionary Settings, M. Colpron, T. Bissig, B.G. Rusk, and J.F.H. Thompson (eds.), Society of Economic Geologists, Special Publication Number 17, p. 53-109.

Pearce, J.A., Harris, N.B.W., and Tindle, A.G., 1984. Trace element discrimination diagrams for the tectonic interpretation of granitic rocks. Journal of Petrology, vol. 25, p. 956-983.

Pigage, L.C., 2004. Preliminary geology of NTS 95D/8 (north Toobally Lakes area), southeast Yukon (1:50 000 scale). Yukon Geological Survey, Open File 2004-19.

Pigage, L.C., 2006. Stratigraphy summary for southeast Yukon (95D/8 and 95C/5). *In:* Yukon Exploration and Geology 2005. D.S. Emond, G.D. Bradshaw, L.L. Lewis, and L.H. Weston (eds.), Yukon Geological Survey, p. 267-285.

Pigage, L.C., 2008. Preliminary bedrock geology for NTS 95D/6 (Otter Creek area), southeast Yukon. *In:* Yukon Exploration and Geology 2007, D.S. Emond, L.R. Blackburn, R.P. Hill, and L.H. Weston (eds.), Yukon Geological Survey, p. 237-255.

Pigage, L.C., 2009. Bedrock geology of NTS 95C/5 (Pool Creek) and NTS 95D/8 map sheets, southeast Yukon. Yukon Geological Survey, Bulletin 16.

Pigage, L.C., Abbott, J.G., and Roots, C.F., 2011. Bedrock geology of Coal River map area (NTS 95D), Yukon (1:250 000 scale). Yukon Geological Survey, Open File 2011-1.

Pigage, L.C. and Anderson, R.G., 1985. The Anvil plutonic suite, Faro, Yukon Territory. Canadian Journal of Earth Sciences, vol. 22, p. 1204-1216.

Pigage, L.C., Crowley, J.L., Pyle, L.J., Abbott, J.G., Roots, C.F., and Schmitz, M.D., 2012. U-Pb zircon age of an Ordovician tuff in southeast Yukon: implications for the age of the Cambrian-Ordovician boundary. Canadian Journal of Earth Sciences, vol. 49, p. 732-741.

Rasmussen, K.L., 2013. The timing, composition, and petrogenesis of syn- to post-accretionary magmatism in the northern Cordilleran miogeocline, eastern Yukon and southwestern Northwest Territories. Unpublished PhD thesis, University of British Columbia, 788 p.

Rasmussen, K.L. and Arehart, G.B., 2010. Preliminary O-S isotopic compositions of Cretaceous granitoids in the Cassiar Platform and Selwyn Basin, Yukon and Northwest Territories. *In:* Yukon Exploration and Geology 2009. K.E. MacFarlane, L.H. Weston, and L.R. Blackburn (eds.), Yukon Geological Survey, p. 279-292.

Rasmussen, K.L., Mortensen, J.K., and Arehart, G.B., 2010. Radiogenic and stable isotopic compositions of mid-Cretaceous intrusions in the Selwyn basin, Yukon and Northwest Territories. Geo-Canada 2010 - Working with the Earth. Canadian Society of Petroleum Geologists, Joint annual convention, Calgary Alberta. Extended abstract. <*www.cspg.org/documents/Conventions/Archives/Annual/2010/0730_GC2010_Radiogenic_and_Stable_Isotopic_Compositions.pdf*> [accessed May 9, 2012]

Rasmussen, K.L., Mortensen, J.K., and Falck, H., 2006. Geochronological and lithogeochemical studies of intrusive rocks in the Nahanni region, southwestern Northwest Territories and southeastern Yukon. *In:* Yukon Exploration and Geology 2005. D.S. Emond, G.D. Bradshaw, L.L. Lewis, and L.H. Weston (eds.). Yukon Geological Survey, p. 287-298.

Rasmussen, K.L., Mortensen, J.K., Falck, H., and Ullrich, T.D., 2007. The potential for intrusion-related mineralization within the South Nahanni MERA area, Selwyn and Mackenzie Mountains, Northwest Territories. *In:* Mineral and energy resource assessment of the Greater Nahanni Ecosystem under consideration for the expansion of the Nahanni National Park Reserve, Northwest Territories. Geological Survey of Canada, Open File 5344, p. 203-278.

Schmitz, M.D. and Schoene, B., 2007. Derivation of isotope ratios, errors and error correlations for U-Pb geochronology using ^{205}Pb-^{235}U-(^{233}U)-spiked isotope dilution thermal ionization mass spectrometric data. Geochemistry, Geophysics, Geosystems, vol. 8, p. Q08006, doi:10.1029/2006GC001492.

Smith, M., 2000. The Tintina gold belt: an emerging gold district in Alaska and Yukon. *In:* The Tintina Gold Belt: Concepts, Exploration, and Discoveries. British Columbia and Yukon Chamber of Mines, Cordilleran Roundup, Special Volume 2, Vancouver, BC, p. 1-3.

Streckeisen, A., 1976. To each plutonic rock its proper name. Earth-Science Reviews, vol. 12, p. 1-33.

Streckeisen, A. and Le Maitre, R.W., 1979. A chemical approximation to the modal QAPF classification of the igneous rocks. Neues Jarbuch fuer Mineralogie Abhandlungen, vol. 136, p. 169-206.

Woodsworth, G.J., Anderson, R.G., and Armstrong, R.L., 1991. Plutonic regimes. *In*: Geology of the Cordilleran Orogen in Canada, H. Gabrielse and C.J. Yorath (eds.), Geological Survey of Canada, vol. 4, p. 491-531.

APPENDIX

SAMPLE DESCRIPTIONS

GUSTY (SAMPLE GUSTY LAKE)

The sample is an unfoliated, medium to fine-grained, porphyritic hornblende-biotite tonalite. Euhedral biotite, hornblende, plagioclase and quartz phenocrysts and glomerocrysts are disseminated in a fine-grained matrix. K-feldspar occurs only in the matrix, constituting up to 20% of the matrix.

KOSTIUK (SAMPLE 09RAS062)

The sample is an unfoliated biotite-hornblende-plagioclase-quartz granodiorite. It is medium grained with a slightly porphyritic to equigranular texture. Staining suggests that the matrix contains 30-40% interstitial K-feldspar. Locally it is extensively altered and contains sericite, epidote and chlorite.

LAST 2 (SAMPLE 09LP098)

The sample is an unfoliated, porphyritic, plagioclase-hornblende granodiorite. Subhedral plagioclase phenocrysts are up to 2 mm across. Rare subrounded and embayed quartz phenocrysts are also present. The matrix consists of a fine-grained mixture of opaques, chlorite, plagioclase, quartz and minor interstitial K-feldspar.

JORGENSEN (SAMPLE 09RAS136)

Texturally the sample is porphyritic with subhedral to euhedral plagioclase, biotite, hornblende, and rare quartz phenocrysts in a fine-grained, unfoliated, interstitial matrix. Compositionally the sample is a quartz monzodiorite. Very minor K-feldspar occurs only in the matrix. Quartz phenocrysts are locally embayed. Locally primary minerals are replaced by epidote, chlorite, sericite and carbonate.

CARIBOU (SAMPLE 09TOA180)

The sample is porphyritic with abundant euhedral to subhedral phenocrysts of plagioclase, biotite, hornblende, and minor quartz in a fine-grained, equigranular matrix. Phenocrysts constitute 50% of the sample. Quartz phenocrysts are rounded and locally embayed. The sample is extensively altered with alteration minerals including sericite, chlorite and epidote. K-feldspar is not present in the sample.

LOOKOUT (SAMPLE 09TOA179)

The sample is a porphyritic granodiorite with euhedral to subhedral biotite and plagioclase phenocrysts in a fine-grained, light grey matrix. The matrix is a mixture of quartz, chlorite and sericite. It is extensively altered; plagioclase is replaced by carbonate, and biotite is replaced by chlorite and carbonate. K-feldspar was not noted in the sample.

SPORK 1 (SAMPLE 10TOA014)

The sample is a coarse-grained, slightly foliated, medium grey, biotite granodiorite. K-feldspar forms large, irregular grains with well-developed microcline grid twinning. In some areas K-feldspar grains have a perthitic texture. The mafic mineral is biotite partially replaced by chlorite-epidote-sphene aggregates, constituting approximately 15% of the mode.

SPORK 2 (SAMPLE 10TOA016)

The sample is a coarse-grained, unfoliated, equigranular, hornblende-biotite quartz diorite. Dark green, subhedral hornblende is intergrown with lesser biotite. Biotite is preferentially replaced by chlorite. Minor quartz occurs as small interstitial grains. K-feldspar is not present, and plagioclase is not altered.

GABE (SAMPLE 09LP048)

The sample is a slightly foliated, equigranular, coarse-grained biotite-muscovite granodiorite. Biotite is intergrown with lesser muscovite; these aggregates partly to completely enclose euhedral to subhedral epidote.

OUDDER (SAMPLE 09TOA135)

The sample is a medium-grained, equigranular to slightly porphyritic, biotite-hornblende granodiorite. Plagioclase forms large subhedral phenocrysts and glomerocrysts in a matrix of interstitial plagioclase and K-feldspar. The rock is fresh with no deuteric alteration.

MAIN (SAMPLE10TOA019)

The sample is a medium-grained, equigranular, foliated, medium grey, muscovite-tourmaline-garnet granite. The feldspar is exclusively plagioclase. Subhedral plagioclase and interstitial quartz constitute approximately 90% of the mode. Staining reveals very minor, fine-grained, interstitial K-feldspar.

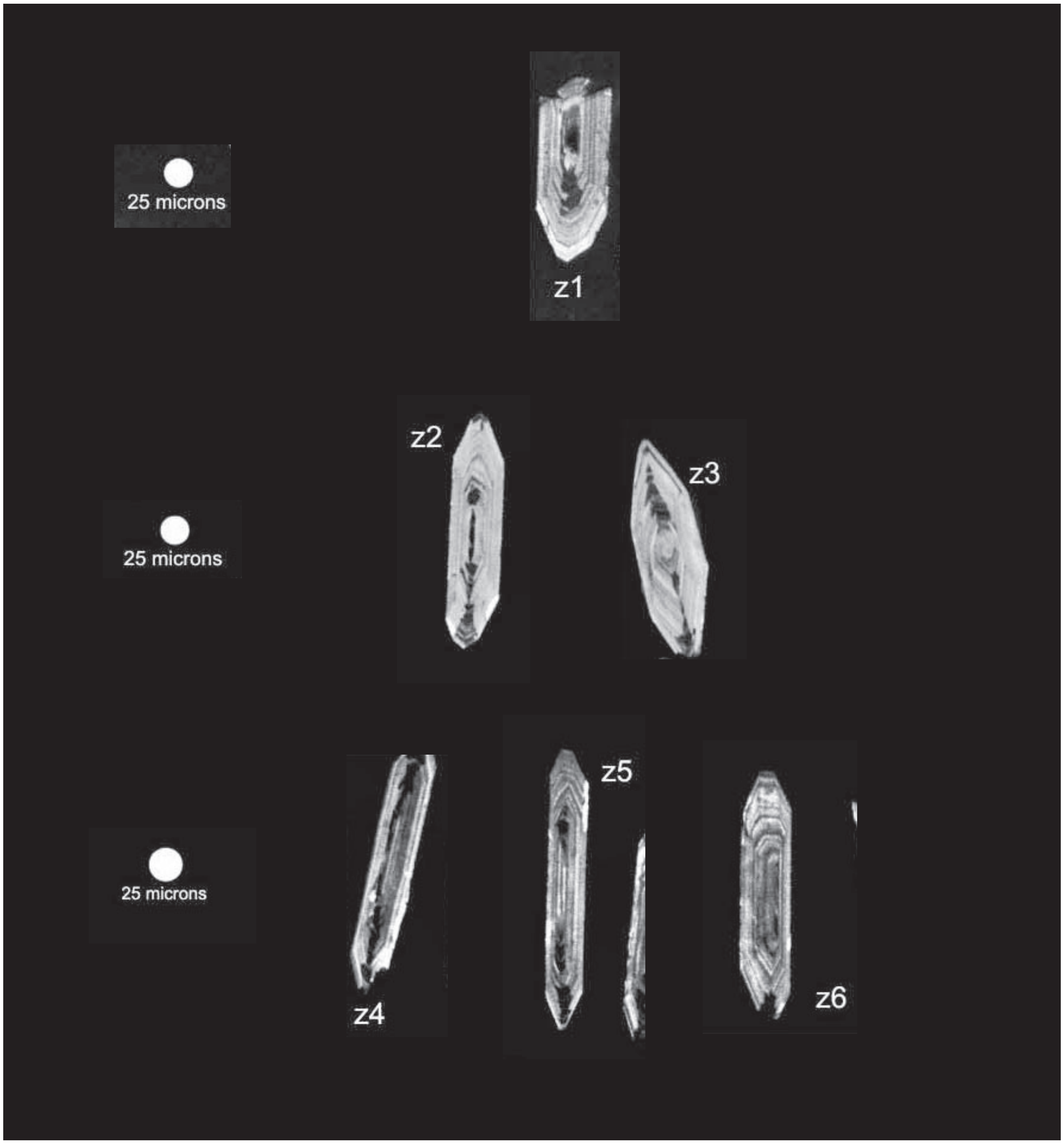

Figure A1. *Cathodoluminescent(CL) images of zircon grains from Jorgensen intrusion (sample 09RAS136).*

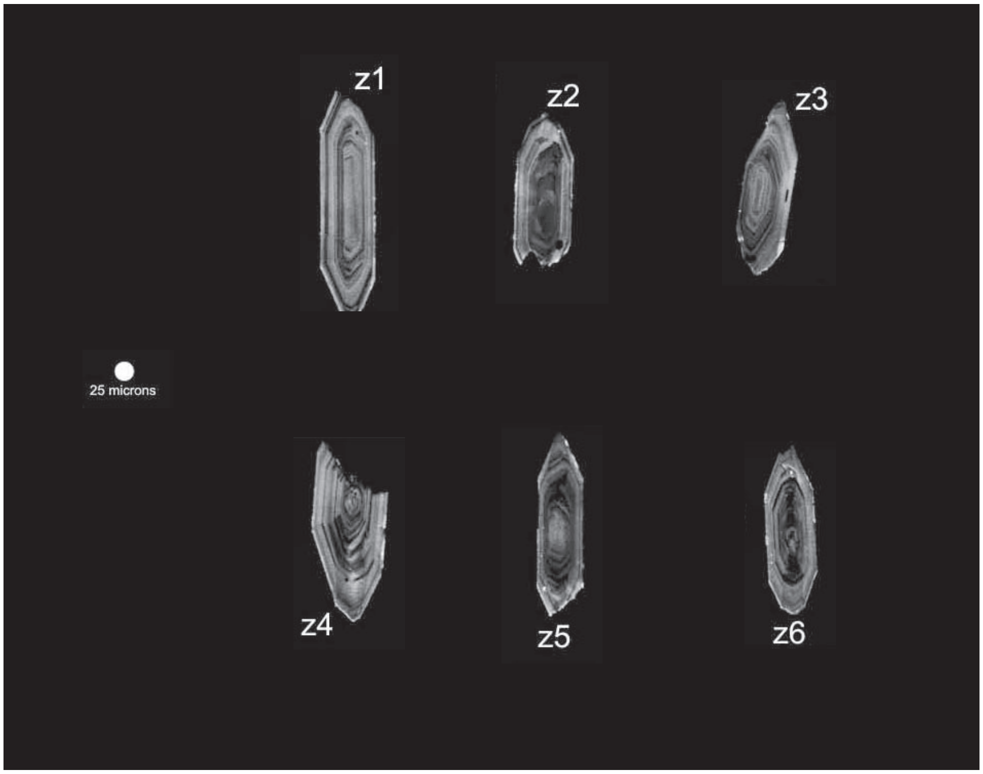

Figure A2. *CL images of zircon grains from Last 2 intrusion (sample 09LP098).*

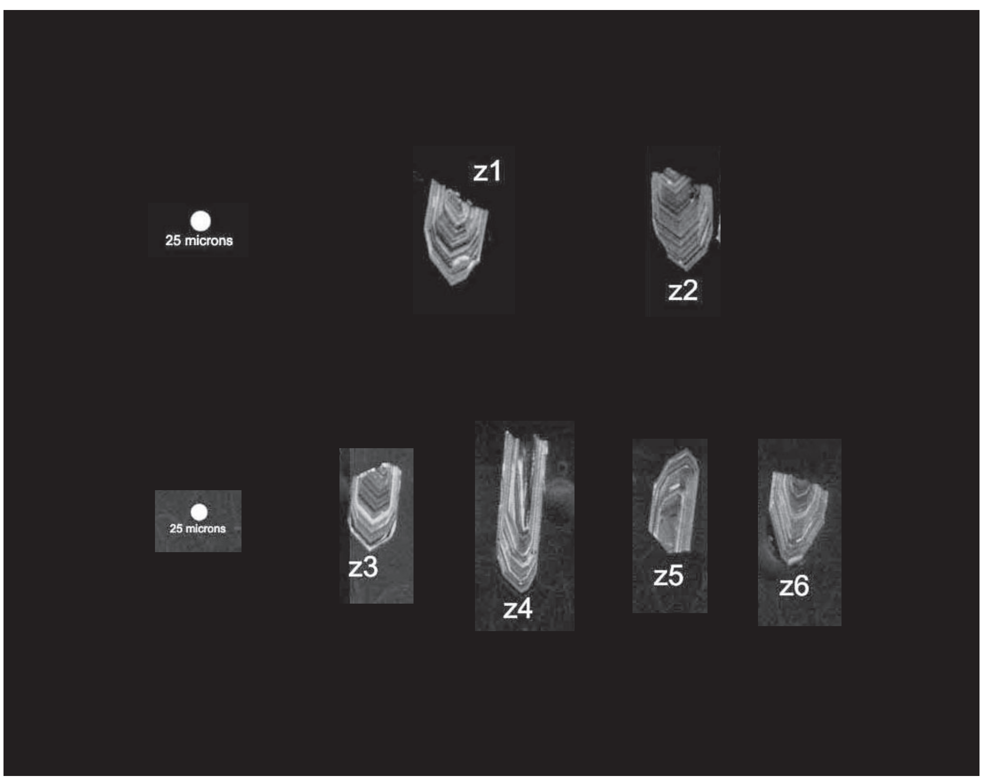

Figure A3. *CL images of zircon grains from Gabe intrusion (sample 09LP048).*

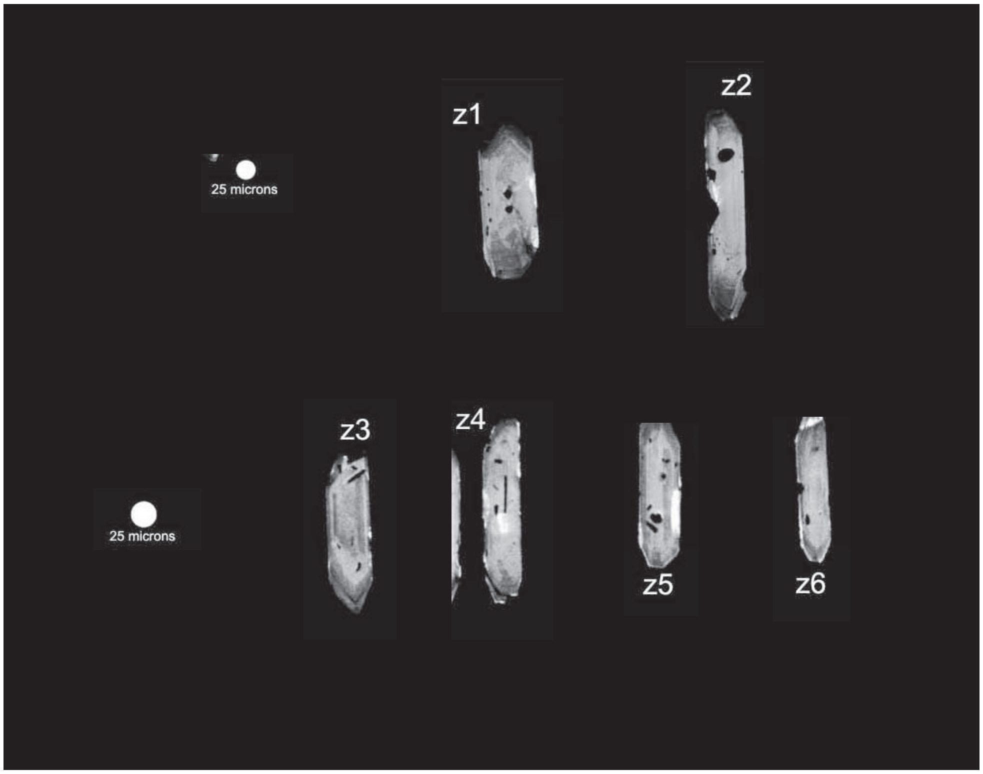

Figure A4. *CL images of zircon grains from Kostiuk intrusion (sample 09RAS062).*

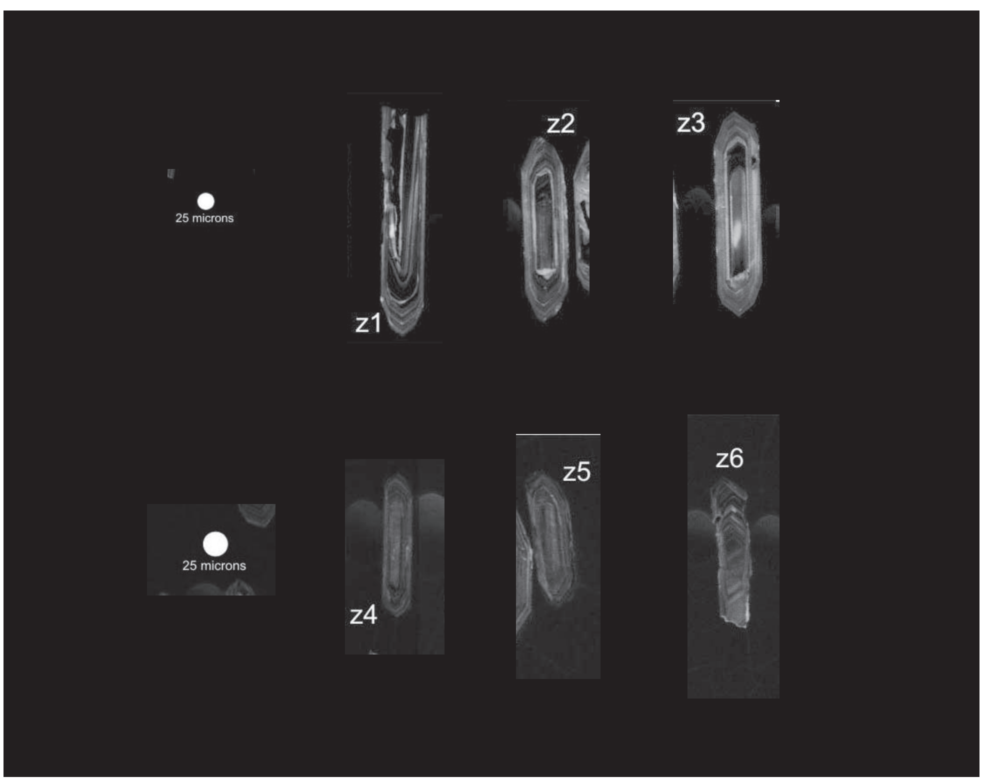

Figure A5. *CL images of zircon grains from Oudder intrusion (sample 09TOA135).*

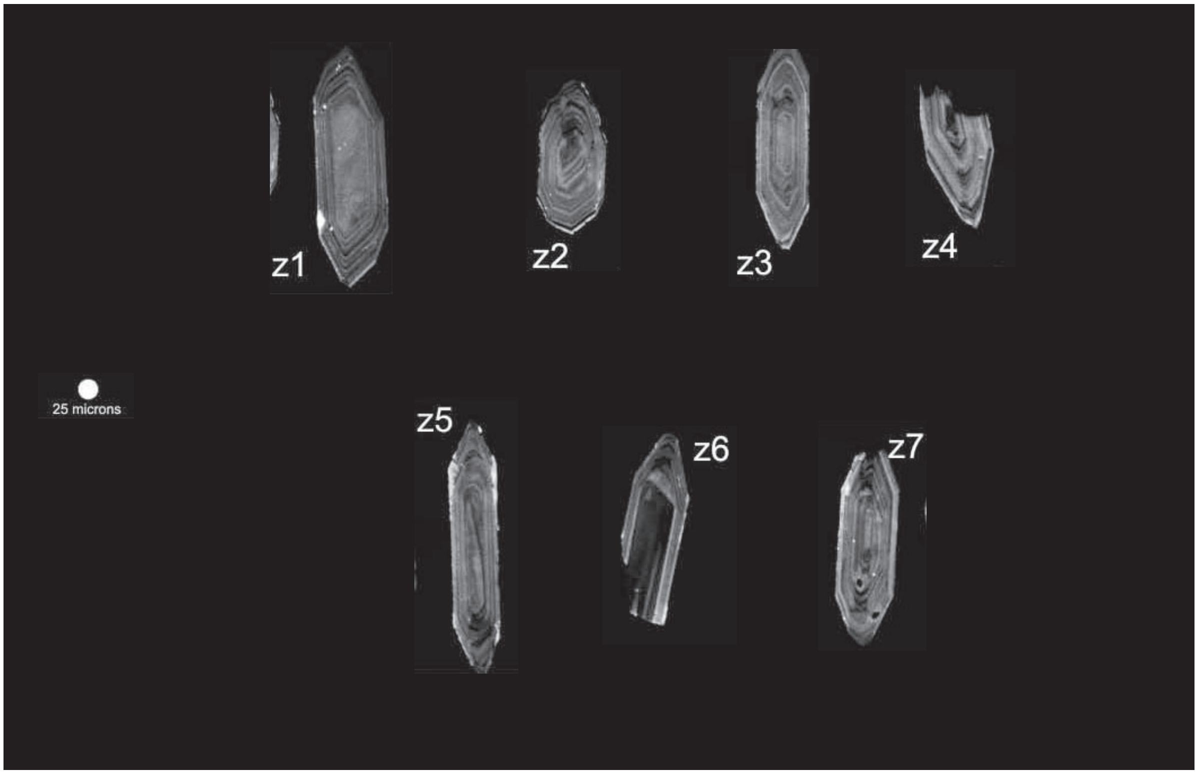

Figure A6. *CL images of zircon grains from Lookout intrusion (sample 09TOA179).*

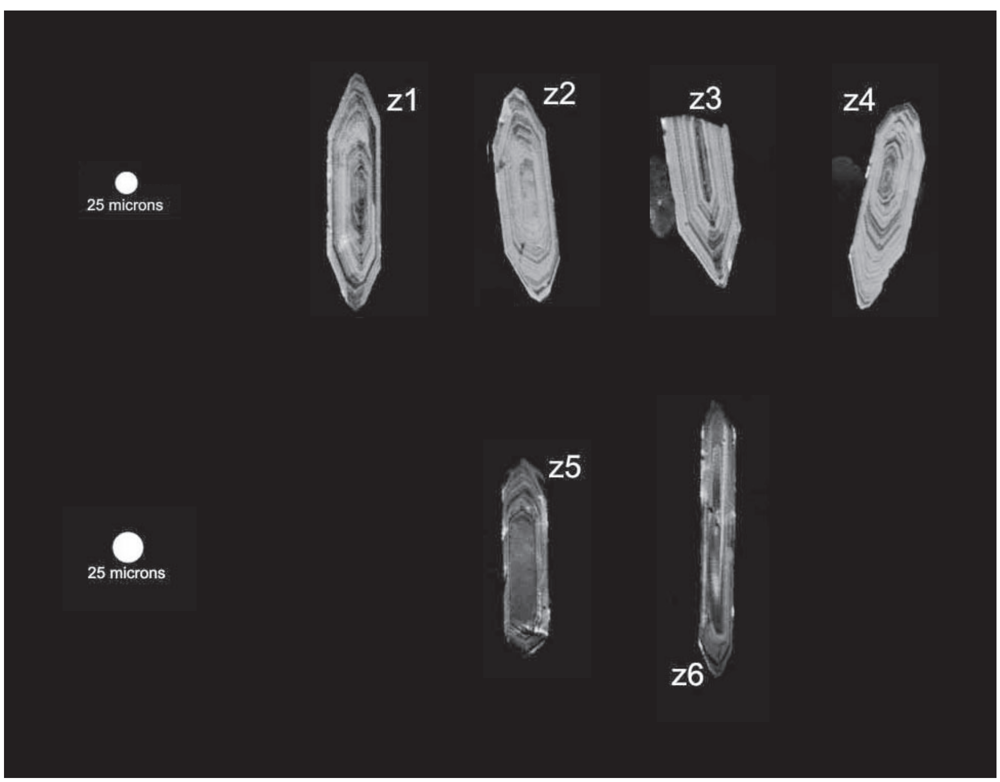

Figure A7. *CL images of zircon grains from Caribou intrusion (sample 09TOA180).*

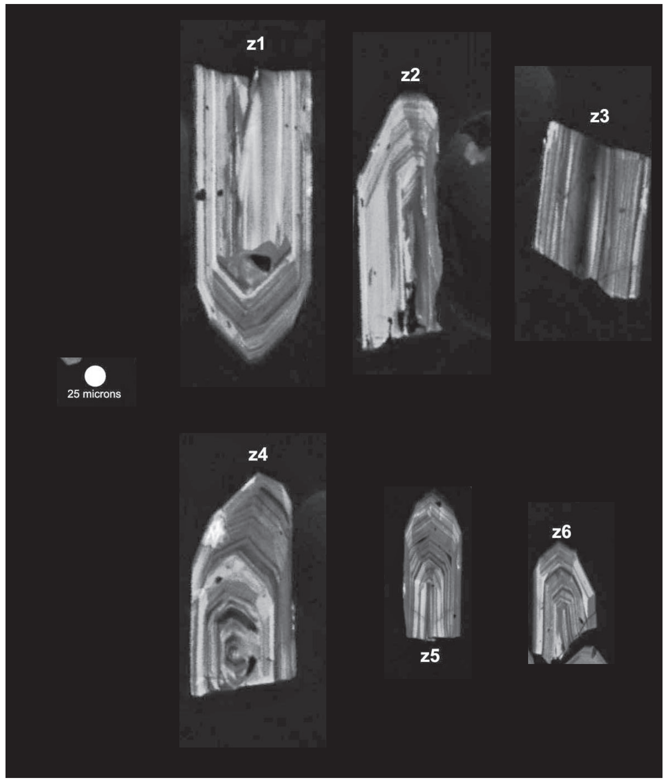

Figure A8. *CL images of zircon grains from Spork 1 intrusion (sample 10TOA014).*

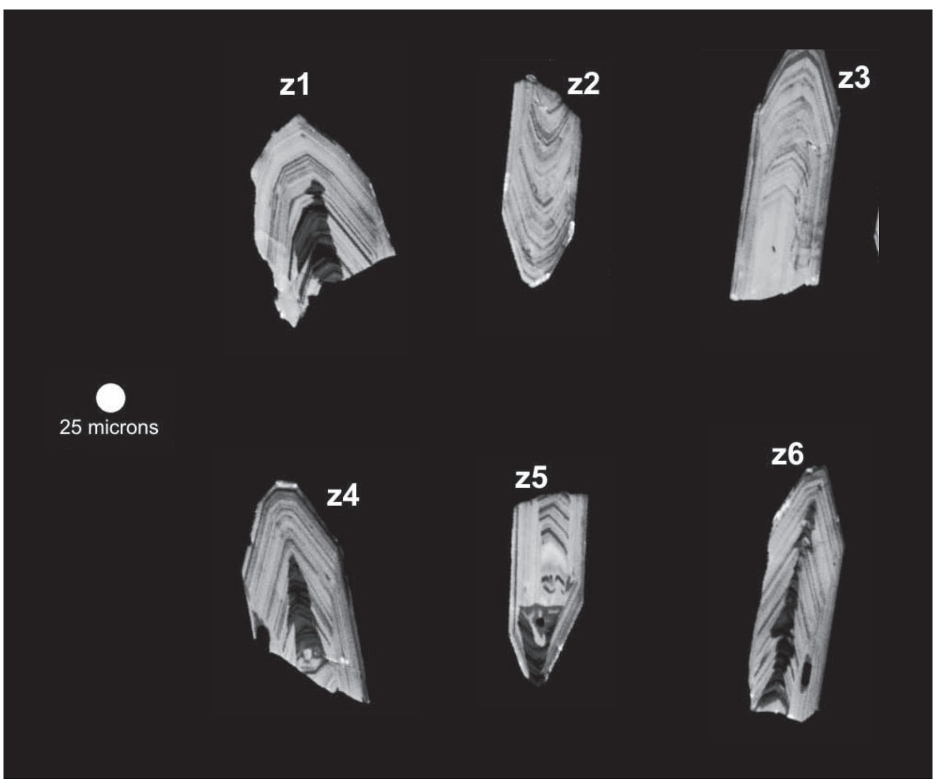

Figure A9. *CL images of zircon grains from Gusty intrusion (sample Gusty Lake).*